Promiscuous and specific bacterial symbiont acquisition in the amoeboid genus Nuclearia (Opisthokonta)

Dirren, Sebastian ; Posch, Thomas

Abstract: We isolated 17 strains of the amoeboid genus Nuclearia (Opisthokonta) from five Swiss lakes. Eight of these nucleariid isolates were associated with bacterial endosymbionts and/or ectosymbionts. Amoebae were characterized morphologically and by their 18S rRNA genes. Phylogeny based on molecular data resulted in four established monophyletic branches and two new clusters. A heterogeneous picture emerged by highlighting nucleariids with associated bacteria. Apart from one cluster which consisted of only isolates with and three groups of amoebae without symbionts, we also found mixed clusters. The picture got even more 'blurred' by regarding the phylogeny of symbiotic bacteria. Although seven different bacterial strains could be identified, it seems that we still are only scratching the surface of symbionts' diversity. Furthermore, types of symbioses might be different depending on host species. Strains of Nuclearia thermophila harboured the same endosymbiont even when isolated from different lakes. This pointed to a specific and obligate interaction. However, two isolates of N. delicatula were associated with different endosymbiotic bacteria. Here the symbiont acquisition seemed to be rather promiscuous. This behaviour regarding symbiotic associations is especially remarkable considering the phylogenetic position of these basal opisthokonts.

DOI: https://doi.org/10.1093/femsec/fiw105

Promiscuous and specific bacterial symbiont acquisition in the amoeboid genus *Nuclearia* (Opisthokonta)

Sebastian Dirren and Thomas Posch[1]

Limnological Station, Department of Plant and Microbial Biology, University of Zurich,

Seestrasse 187, CH-8802 Kilchberg, Switzerland

Running Title: Bacterial symbionts of *Nuclearia*

Number of pages (incl. references & figure legends): 33

Number of tables: 2

Number of figures: 7

Number of Supplementary Figures: 3 (merged in one docx-file)

Intended as Research Article in FEMS Microbiology Ecology

[1]Corresponding author:
PD Dr. Thomas Posch
Limnological Station, Department of Plant and Microbial Biology, University of Zurich
Seestrasse 187, CH-8802 Kilchberg, Switzerland
Phone: 0041 44 634 9224
Fax: 0041 44 634 9225
e-mail: posch@limnol.uzh.ch

Abstract

We isolated 17 strains of the amoeboid genus *Nuclearia* (Opisthokonta) from five Swiss lakes. Eight of these nucleariid isolates were associated with bacterial endo- and /or ectosymbionts. Amoebae were characterized morphologically and by their 18S rRNA genes. Phylogeny based on molecular data resulted in four established monophyletic branches and two new clusters. A heterogeneous picture emerged by highlighting nucleariids with associated bacteria. Apart from one cluster which consisted of only isolates with and three groups of amoebae without symbionts, we also found mixed clusters. The picture got even more 'blurred' by regarding the phylogeny of symbiotic bacteria. Although seven different bacterial strains could be identified, it seems that we still are only scratching the surface of symbionts' diversity. Furthermore, types of symbioses might be different depending on host species. Strains of *N. thermophila* harboured the same endosymbiont even when isolated from different lakes. This pointed to a specific and obligate interaction. However, two isolates of *N. delicatula* were associated with different endosymbiotic bacteria. Here the symbiont acquisition seemed to be rather promiscuous. This behaviour regarding symbiotic associations is especially remarkable considering the phylogenetic position of these basal opisthokonts.

Introduction

Intimate associations between unicellular or invertebrate eukaryotes and prokaryotes are ubiquitous and their importance for the evolution of 'higher' life forms is increasingly recognized (Smith 1989; McFall-Ngai *et al.* 2013; Alegado and King 2014; Kiers and West 2015). We can intuitively argue that the probability of interactions increases, if the spatial distance between hosts and potential symbionts is small, which is often the case for protists and bacteria. Knowing that such interactions are manifold, we use the term symbiosis in a very general way. We call the phenomenon of a close association of dissimilar organisms a 'symbiosis', thus we follow the original definition of this term by de Bary (see Appendix1 in Paracer and Ahmadjian 2000). On an evolutionary scale, symbioses between eukaryotes and prokaryotes may emerge and disintegrate constantly and only a minute part will turn into 'stable associations'. The most stated and intensively studied examples are mitochondria and plastids that originated from the endosymbiosis of a host cell with alphaproteobacteria (Thrash *et al.* 2011) and cyanobacteria (Rodríguez-Ezpeleta *et al.* 2005), respectively. Beside the fundamental functions of respiration and photosynthesis, we know several traits which bacterial symbionts may provide to their eukaryotic hosts, e.g. they can be important for the host's nutrition, defence, competition, and adaption to the environment (Gast *et al.* 2009). Associated bacteria can also be involved in the production (Freeman *et al.* 2012) or degradation of secondary metabolites including toxins (Kikuchi *et al.* 2012; Dirren *et al.* 2014).

Here we focus on members of the amoeboid genus *Nuclearia* (Opisthokonta, Nucleariidae) which can live in symbiosis with ecto- and endosymbiotic bacteria. *Nuclearia* is a single genus in the family Nucleariidae which is a sister group to Fungi (Zettler *et al.* 2001; Steenkamp *et al.* 2006; Liu *et al.* 2009). As far as we know, there is only one documented case of an opisthokont protists with prokaryotic symbionts. Wylezich *et al*. (2012) described the chanoflagellate *Codosiga balthica*, which harboured two different endosybiotic bacteria

43 inside the cytoplasm. This lack of evidence is remarkable considering the importance of
44 symbiotic interactions for multicellular opisthokonts. Nucleariid amoebae are usually
45 surrounded by a glycocalyx (Moran *et al.* 2011; Ouwerkerk *et al.* 2013), which can be
46 colonized by ectosymbiotic bacteria (Artari 1889; Cann and Page 1979; Patterson 1984; Cann
47 1986). In a previous study we characterized *Nuclearia* sp. strain N (hereafter named *N.*
48 *thermophila* strain N) which harboured the bacterial ectosymbiont (*Paucibacter toxinivorans*)
49 nicely arranged inside the glycocalyx (Dirren *et al.* 2014). The interaction between *N.*
50 *thermophila* strain N and this prokaryote seemed to be specific and stable.
51 Multicellular organisms usually are associated with more than one bacterial species.
52 Ectosymbionts form entire assemblages which are designated as microbiota of the respective
53 host. The microbiota of very 'simple' animals like the cnidarians *Hydra* (Fraune and Bosch
54 2007; Franzenburg *et al.* 2013) and corals (Lema *et al.* 2014) seem to be relatively distinct
55 and even species-specific. In higher animals including humans (Huttenhower *et al.* 2012) the
56 microbiota is more diverse and variations between individuals within the same population are
57 pronounced. However, in contrast to the taxonomic variability, the functional roles of such
58 assemblages seem to be conserved. Thus, composition and function of the microbiota is
59 essential for the organism's well-being. A multitude of diseases are consequently caused by
60 regime shifts to unhealthy and unstable states (Lozupone *et al.* 2012). The 'simplicity' of the
61 *Nuclearia* system could be a great benefit for the fundamental understanding of interactions
62 of prokaryotes with their opisthokont hosts.
63 Symbiotic interactions of Nucleariidae are not restricted to ectosymbiotic associations
64 but amoebae may additionally harbour bacterial endosymbionts. For example, *N. radians*
65 (described as *Nucleosphaerium tuckeri* by Cann and Page (1979)) may be associated with
66 ecto- as well as endosymbiotic bacteria. In recent studies, the rickettsial endosymbiont of *N.*
67 *pattersoni* (Dykova *et al.* 2003) and *Candidatus* Endonucleariobacter rarus (Dirren *et al.*
68 2014) of *N. thermophila* strain N were characterized. Endosymbiotic bacteria are not at all as

common in higher life forms as ectosymbionts. The barrier for bacteria to enter metazoans' cells is rather rigid and well protected (e.g. by the immune system). In vertebrates mainly pathogens are able to enter cells causing infections and pathological states (Casadevall 2008). From an evolutionary point of view this is of great interest as multicellular organisms seem to 'outsource' their bacterial associations to preserve their integrity. Consequently the glycocalyx can be regarded as a kind of 'external organ' harbouring the symbiotic assemblage. This arrangement not only allows benefiting from the microbiota but ensures a minimal physical distance and thus protection (Fraune *et al.* 2015).

To sum up, from a phylogenetic perspective, Nucleariidae might be good model organisms to verify hypotheses about symbioses in general. In order to study these interactions it is the first step to elucidate the diversity of Nucleariidae and to characterize in parallel their symbionts. In this study (i) we report on the morphology and taxonomic affiliation (18S rRNA genes) of 17 *Nuclearia* strains. (ii) All isolates were screened for bacterial symbionts both in the glycocalyx and inside amoebae. (iii) Finally, we focused on symbionts of *N. delicatula* and *N. thermophila* strains, and analysed the ultrastructure and the intracellular localisation of endosymbiotic bacteria via transmission electron microscopy (TEM). Additionally we sequenced the bacterial 16S rRNA genes for phylogenetic analyses.

Key words: Bacteria-protist symbioses; Ectosymbionts; Endosymbionts; *Nuclearia*; Nucleariidae; Glycocalyx

Methods

Strains and cultures

Seventeen *Nuclearia* strains were isolated from benthic and pelagic water samples of five Swiss lakes (Table 1). Single cells were picked with a glass-pipette and washed in sterile water to generate monoclonal xenic amoebal cultures. Finally, isolates were cultured in autoclaved mineral water (Cristalp) and the cyanobacterium *Planktothrix rubescens* was added as sole food source. *P. rubescens* BC 9307 was isolated from Lake Zurich (Walsby *et al.* 1998) and is kept as axenic stock culture. *Nuclearia* cultures were maintained at a 12 h light (irradiance: 5-15 µmol m^{-2} s^{-1}) / 12 h dark cycle in Tissue Culture Flasks 25 cm^2 (TPP®) at 18° C. Cultures were fortnightly renewed by adding 1 ml of the axenic cyanobacterial stock culture to 10 ml of new culture medium inoculated with 200 µl of an older culture. For all analyses, we included the dataset about *N. thermophila* strain N and its bacterial ectosymbiont *Paucibacter toxinivorans* strain SD41 (HG792253), originating from our previous study (Dirren *et al.* 2014). *N. delicatula* strain G (CCAP 1552/6), *N. moebiusi* strain K (CCAP 1552/7), *N. thermophila* strain N (CCAP 1552/5) and *N. pattersoni* strain A2 (CCAP 1552/8) were deposited in the Culture Collection of Algae and Protozoa (CCAP).

Morphological analysis and cladistic tree

Morphological characters were observed by light microscopy on living specimens. Features like multinucleate / uninucleate, evident / not evident nucleolus and branching of filopodia were observed when cells adapted a flattened form under the compression of the cover slip. Cells were considered 'spherical' if floating individuals in the water column could be observed (even if they were not always 'perfect' spheres). Strains were classified as being able to adapt a 'flattened form' when cells have ever attached to and moved on surfaces. The formation of syncytia was defined as the fusion of two or more cells. In addition we checked all culture flasks for the appearance of cysts. The glycocalyx was either seen with phase

contrast as translucent halo surrounding cells or after staining with Alcian blue. Ectosymbionts were defined as bacteria inside the glycocalyx located close to the cell membrane (loosely attached bacterial cells on the outer border of the glycocalyx were not classified as symbionts). Endosymbionts were detected with epifluorescence microscopy after DAPI staining and by *in situ* hybridization (CARD-FISH). The body diameter of spherical cells was measured more than three months after isolation of the strains. Only for *N. thermophila* strain D6 additional measurements were taken right after isolation. For calculations of the cladistic tree, morphological characters were judged as either present or absent and each strain was attributed to one of three size classes: 1. $x < 13$ µm; 2. 13 µm $< x <$ 20 µm; 3. $x > 20$ µm. The cladistic tree (Jaccard's similarity coefficient) was calculated with the Add-In software XLSTAT (Addinsoft™).

Sequencing of the 18S rRNA genes (Nucleariidae)

DNA was extracted from aliquots (1.5 ml) of *Nuclearia* cultures with the GenElute™ Bacterial Genomic DNA Kit (Sigma). PCR with GoTaq® Green Master Mix (Promega) and the eukaryote-specific primers Euk328f and Euk329r (Moon-van der Staay *et al.* 2001) was used to amplify the 18S rRNA genes. If gel elecrophoresis resulted in the detection of bands of expected size, PCR products were purified with QIAquick PCR Purification Kit (Qiagen) and Sanger sequenced with ABI BigDye chemistry on an ABI 3130x Genetic Analyzer (Applied Biosystems). In order to sequence the entire amplicons, the additional primers SR2f, SR2r, SR4f, SR6f, SR6r, SR8f, SR8r, SR10f and SR10r (Nakayama *et al.* 1998) were used. In seven cases (strains G, D, S4, D4, B6, B1 and B3) the direct sequencing was not successful. Here 18S rRNA genes were again amplified from the extracted DNA with Platinum® PCR Super Mix High Fidelity (Invitrogen) and the primers Euk328f and Euk329r. Subsequently, PCR products were purified as mentioned above and cloned into *Escherichia coli* using a pGem®-T Vector (Promega) according to the manual. Clones were screened for expected size

inserts with the plasmid primers M13f and M13r. Positive clones were grown in liquid cultures and plasmids were purified with GenElute™ Five-Minute Miniprep Kit (Sigma). Inserts of plasmids were sequenced in the same way as PCR products but plasmid primers were used instead of Euk328f and Euk329r.

Sequencing of the 16S rRNA genes (symbionts)

Two 16S rRNA gene clone libraries were constructed from *N. delicatula* strain D and strain G, respectively. About 130 *Nuclearia* cells were picked with a micropipette and washed in sterile water. After three freeze-thaw cycles DNA was extracted with GenElute™ Bacterial Genomic DNA Kit (Sigma). Extracted DNA served than as template for amplification of 16S rRNA genes with Platinum® PCR Super Mix High Fidelity (Invitrogen) and the primers GM3f and GM4r (Muyzer and Ramsing 1995). After purification of PCR products and ligation into the pGem®-T Vector (Promega) they were cloned following the manufacturer's protocol. Positive *E. coli* clones were detected by screening with plasmid primers (size ~1.6 kbp) and their plasmids purified as described above. Sequencing of inserts was done with plasmid primers and the additional primer GM1f (Muyzer and Ramsing 1995). Partial 16S rRNA genes of the endosymbiont *Candidatus* Endonucleariobacter rarus from *N. thermophila* strain A and strain D6 were sequenced directly. The sequence of the probe CoNuc67 (Table 2) was used to design a specific primer (P1_CoNuc_f 5'-TAACAGAGTGTGTAGC-3'). PCR amplification with GoTaq® Green Master Mix (Promega) was done with extracted DNA from these cultures using the forward primer P1_CoNuc_f and the revers primer GM4r (positive control: ext. DNA from *N. thermophila* strain N; negative control: ext. DNA from *N. thermophila* strain B1). Subsequently purified PCR products were directly sequenced with the primers P1_CoNuc_f and GM4r as described above (LN875086-LN875088).

Phylogenetic analyses

The software DNA Baser v3.5.0 (Heracle BioSoft) served as tool for assembling partial sequences. Chimeric sequences were detected and removed using Mallard and Pintail (Ashelford *et al.* 2005). For phylogenetic analyses the ARB software package (Ludwig *et al.* 2004) with the SILVA database SSU Ref 111 (Pruesse *et al.* 2007) was used.

All available *Nuclearia* 18S rRNA gene sequences from described species, our isolates, and as outgroup two sequences from *Candida* sp. (AB013586 and EU348785) were included for phylogenetic tree reconstruction. Sequences were trimmed and aligned with the MAFFT aligner (Katoh and Standley 2013). Alignments were manually optimized and ambiguous regions (e.g. insertions in the V4; V7 and V8 domains) were removed resulting in 1501 positions with 150 distinct alignment patterns. Another phylogenetic tree including all our *N. delicatula* clones, *N. delicatula* (AF349563) and *N. simplex* (AF349566) / *N. moebiusi* (AF349565) as outgroup was calculated. Sequences were aligned and trimmed as discribed above but none of the hypervariable regions was removed (2363 positions with 204 distinct alignment patterns).

The 16S rRNA gene sequences of symbionts were aligned with the SINA web aligner (www.arb-silva.de/aligner/). Five phylogenetic trees (*Ca.* Endonucleariobacter rarus: 1305 positions, 56 distinct patterns; ectosymbionts: 1417 positions, 199 distinct patterns; endosymbionts: 1558 positions, 827 distinct patterns; clone library strain G: 1383 positions, 617 distinc patterns; clone library strain D: 1415 positions, 769 distinct patterns) were calculated with our sequences and related sequences from the SILVA database (quality scores ≥ 88).

For the reconstruction of phylogenetic trees Maximum Likelihood (ML) and Bayesian inference (BI) methods were used. Bootstrapped ML trees were calculated (1000 iterations) using the RAxML algorithm (Stamatakis *et al.* 2008). The parameters were: GTR (General Time Reversible) model with a Γ distribution for rate heterogeneity among sites, with 4

discrete rate categories. BI was calculated using the ExaBayes software package (©The Exelixis Lab). The posterior probabilities from BI trees (4 chains; 100000 generations) were added to ML trees where trees of both methods were congruent. Full length 16S rRNA gene sequences from clone libraries and 18S rRNA gene sequences of the *Nuclearia* strains were deposited in the EMBL database with the accession numbers LN875040-LN875170.

CARD-FISH and probe design

First, CARD-FISH with the general probes EUB I-III (Daims *et al.* 1999), ALF968 (Neef 1997), BET42a, GAM42a (Manz *et al.* 1992), CF319a (Manz *et al.* 1996), HGC69a (Roller *et al.* 1994), and VER47 (Buckley and Schmidt 2001) allowed for the identification of symbionts on a higher taxonomical level. Afterwards clusters of potential symbionts were chosen from phylogenetic trees of the 16S rRNA gene clone libraries. Specific probes were designed based on the sequences of these candidate clusters. Probe design with the dedicated ARB tool resulted in four specific CARD-FISH probes (Table 2). The Ribosomal Database Project (www.rdp.cme.msu.edu) and the web tool Mathfish (Yilmaz *et al.* 2011) were used for *in silico* testing of the new probes. Appropriate formamide concentrations (for highest stringency) were determined empirically. Non-specific staining was addressed with the probe NON338 (Wallner *et al.* 1993). CARD-FISH on filters was done with differently labelled tyramids (fluorescein and Alexa546) following the previously published protocol (Dirren *et al.* 2014). In addition, CARD-FISH of amoebae on gelatine-coated glass slides and embedded in agarose were prepared.

Microscopy and photographic documentation

Differential interference and phase contrast images were acquired with a Canon EOS1000D controlled by the software AxioVision 4.8.2 (Zeiss) installed on an Axio Imager.M1 microscope (Zeiss). CARD-FISH preparations were analysed at the same microscope with

epifluorescence microscopy (Zeiss optical filter sets: set 01, 10, 14, and 43) and by confocal laser-scanning microscopy (SP5-R, Leica Microsystems, Germany).

Transmission electron microscopy (TEM)

Glutaraldehyde (final conc. 1.25 %) and osmium tetroxide (final conc. 1 %) were mixed and added to small volumes of *N. delicatula* strain D and strain G cultures (after centrifugation at 1000 g for 20 min and discarding of supernatants). Fixation was done on ice for 1h followed by two washing steps (centrifugation for 10 min at 2000 g and exchanging of fixative solution with H_2O). Washed pellets were re-suspended in melted agar (2 %). After hardening and cutting the agar block into smaller pieces (~10 mm^3) they were block stained with uranylacetat (1 %) for 1h at room temperature. Subsequently, samples were dehydrated in an ethanol series (70 %, 80 %, 96 % and 100 %) and finally in propylenoxide, followed by embedding in epon-araldite. Ultrathin sections were cut with an Ultracut UCT (Leica) and post-stained with lead citrate for 6 min. An electron microscope Philips CM100 equipped with a digital camera (Gatan Orius 1000) was used for the analysis of the TEM preparations.

Results and Discussion

Morphological versus molecular phylogeny of *Nuclearia* spp.

For a long time, nucleariid amoebae were described using only morphological characters. However, the majority of these amoeboid species share many features used for their identification (see Table 1 in Yoshida *et al.* (2009)). It seems that some inadequately defined characters were even interpreted differently by researchers, e.g. if amoebae may form flattened / spherical cells, if a glycocalyx is present or absent and if the nucleolus is evident. This becomes obvious, when comparing Figure 11 in Patterson (1984), where the author stated the lack of a glycocalyx, with Figure 6 in Pernin (1976), where the presence of EPS was proven. In addition to these 'vague' characters, other features like the formation of multinucleate syncytia, cyst production, and the appearance of branched filopodia might be rarely or not at all observed depending on culture and observation conditions. Even the cell size of single isolates may vary depending on culture conditions. We documented at least for one isolate a shrinkage of cells in the course of cultivation. The mean cell size of *N. thermophila* strain D6 decreased from initially 24.6 µm (day 7 after isolation, n=56) to 15.7 µm (day 90, n=100). Thus, most probably these inconsistencies and different interpretations of features led to re-descriptions of species and incorrect identifications.

This assumption is additionally supported by the fact, that two *N. simplex* isolates clustered in the 18S rRNA gene based phylogenetic tree very distantly (Fig. 1A) with *N. moebiusi* and *N. pattersoni*, respectively. Due to this discrepancy we considered the two as *N. simplex* identified isolates to belong to different species. Consequently, we will name these phylogenetic groups: *N. moebiusi* and *N. pattersoni* cluster, respectively. Moreover, two sequences of one and the same *N. moebiusi* isolate (AF349565 and AF484686) were included in phylogenetic trees by some authors (Dykova *et al.* 2003; Yoshida *et al.* 2009) which further caused confusions.

Nevertheless, in this study we partly worked with traditional morphological features for comparisons of our strains (Fig. 2 and Supplementary Fig. S1) with published species descriptions. To characterise our *Nuclearia* spp. isolates we even included four additional features: benthic isolate, pelagic isolate, presence of ectosymbionts, and presence of endosymbionts (Table 1). We checked if the morphological classification corresponded to the molecular phylogeny by performing a cladistic analysis based on presence / absence of characters. The cladistic tree (Fig. 1B) and the 18S rRNA gene based maximum likelihood (ML) tree (Fig. 1A) were in good accordance regarding the *N. delicatula* and the *N. thermophila* clusters. In both trees, they were sister groups including same isolates. In contrast, the third big cluster in the cladistical tree unified isolates from distant branches of the ML tree. Although the substructure of this third cluster reflected quite well the 18S rRNA gene based phylogeny, two isolates clustered differently. In the cladistic tree *Nuclearia* sp. strain NZ had no close relative and strain K formed together with strains A1 and D1 a group, which was not confirmed by molecular phylogeny. Taken together, only *N. delicatula* and *N. thermophila* strains could be identified solely by their morphological traits. For the affiliation of all other isolates additional molecular information (18S rRNA genes) was needed.

Assignment of isolates to described species

The species descriptions of *N. delicatula* from Patterson (1984) and Cann (1986) are in good accordance with morphological features (Table 1) observed for all isolates in the *N. delicatula* cluster.

The morphological features described for *N. moebiusi* differed from what we observed for *Nuclearia* sp. strain K. We found spherical cells as well as a glycocalyx which was not reported for *N. moebiusi*. When considering the ‘excavate cavities’ (Figure 11 from Patterson (1984)) to be the glycocalyx and additionally taking the trait ‘spherical form’ less restrictive, we can assign our isolate to this species (i.e. *N. moebiusi* strain K).

285 The morphological incongruences between *N. thermophila* strain N and the original species
286 description of *N. thermophila* by Yoshida *et al.* (2009) were discussed in our previous study
287 (Dirren *et al.* 2014). For the isolates clustering together with *N. thermophila* we reported a
288 good accordance with the characters earlier described for *N. thermophila* strain N. Only the
289 formation of syncytia could not be documented for strains B1 and D6. The present results
290 including morphological and phylogenetic analyses of four different isolates (strains B1, D6,
291 A, N), thus justify their assignment to the species *N. thermophila.*
292 All the described features for *N. pattersoni* (Dykova *et al.* 2003) except the presence of
293 endosymbionts could be observed for *Nuclearia* sp. strain B4 and A2. Taking their
294 phylogenetic close relatedness (Fig. 1A) into account we can assign them to the species *N.*
295 *pattersoni*.
296 The isolates *Nuclearia* sp. strain NZ, strain A1 and strain D1 built a sister group to the *N.*
297 *pattersoni* cluster (Fig. 1A). Morphologically these three isolates were very similar and the
298 lack of cysts was the only character differentiating them from *N. pattersoni* isolates. However,
299 the phylogenetic distance (Fig. 1A) still does not allow for assigning them to the described
300 species.
301 Finally the two isolates *Nuclearia* sp. strain B3 and A5 formed a discrete new phylogenetic
302 group. In spite of only minor morphological differences (e.g. formation of syncytia in strain
303 A5) to isolates in the *N. moebiusi* and *N. pattersoni* clusters, we suppose that they form a new
304 species. Phylogenetic reconstruction even points at a rather basal position, probably
305 representing a sister group to *N. delicatula*, *N. moebiusi* and *N. thermophila*. We added
306 hypothetical gains and losses of the features ‘cyst production’ and ‘formation of syncytia’ to
307 the corresponding branches (Fig. 1A). The fact that we found cyst production for isolates all
308 over the tree may indicate that the common ancestor was encysting. In contrast the formation
309 of syncytia was found only for isolates in one of the main branches and thus could be an
310 acquired trait.

311 **Variability of the nucleariid 18S rRNA gene copies**

312 For all but seven *Nuclearia* isolates, PCR amplification of the 18S rRNA gene with general
313 eukaryotic primers and direct sequencing was successful (LN875106-LN875114). In contrast,
314 assembling of partial 18S rRNA gene sequences failed for *N. thermophila* strain B1,
315 *Nuclearia* sp. strain B3 and all *N. delicatula* isolates (strains G, D, S4, D4 and B6). For *N.*
316 *thermophila* strain B1 a poly-G region causing 'hard stops' during sequencing resulted in two
317 non-overlapping partial sequences. The first part (~ 700 nt) and the second part (~ 1230 nt) of
318 the 18S rRNA gene could thus not be assembled. Sequence qualities of all *N. delicatula*
319 strains and *Nuclearia* sp. strain B3 dropped in regions containing homopolymers due to
320 superposition of signals. This pointed to sequence variations in multiple 18S rRNA gene
321 copies (e.g. different lengths of homopolymers). Therefore, PCR products of *N. delicatula*
322 strains and *Nuclearia* sp. strain B3 were cloned and de novo sequenced resulting in partial
323 sequences with high quality scores even for regions containing homopolymers. Two to ten
324 different clones were completely sequenced (LN875123- LN875170) for *N. delicatula*
325 isolates and *Nuclearia* sp. strain B3. In order to exclude that inter-clone variation was
326 introduced by PCR and sequencing errors, we re-amplified 18S rRNA genes from cleaned-up
327 plasmids of three *N. delicatula* strain D4 clones. The obtained sequences were identical to
328 those generated by direct sequencing of inserts. Thus, detected inter-clone variations most
329 probably originated from natural variations in 18S rRNA gene copies and were not artefacts.

330 Micro-heterogeneities in the nucleariid 18S rDNA have been already documented by
331 Zettler *et al.* (2001). They mainly originate from size variations in the insertions inside the
332 V4, V7 and V8 domains (sensu De Rijk *et al.* 1992). Pairwise sequence distances were
333 calculated for each clone library of *N. delicatula* strains (G, D, S4, D4), *Nuclearia* sp. strain
334 B3 and *N. thermophila* strain B1 (Supplementary Fig. S2A). Variations in the 18S rRNA gene
335 copies of *N. thermophila* strain B1 (mean ± standard deviation: 0.21±0.07 %) were lower than
336 those in *N. delicatula* strains (0.48±0.15 % to 0.63±0.24 %) and in *Nuclearia* sp. strain B3

(0.44±0.24 %). Intra-strain variations (distances of clone sequences: 0.58±0.05 %) were about three times higher than inter-strain variations (distances of the consensus sequences: 0.17±0.07 %) for *N. delicatula* isolates. Thus, they could not be separated phylogenetically on the base of this marker gene (Supplementary Fig. S2B). When we calculated sequence similarity of *N. delicatula* (AF349563) and *N. delicatula* strain G without these variable parts in the V4, V7 and V8 domains we got a high value of 99.7 %. In contrast, sequence similarity including the hypervariable stretches was only 94 %. In the same way 18S rRNA gene copies in single isolates are mainly diverging (e.g. due to insertion and deletion of nucleotides) inside the homopolymers of hypervariable domains. Slipped-strand mispairing (Levinson and Gutman 1987) might be the mechanism behind this phenomenon. A slightly higher mutation rate could also be detected for the variable stretches in sequences from the *N. pattersoni* cluster (e.g. sequence similarity of the described *N. pattersoni* and *N. pattersoni* strain B4: with homopolymer region 99 % and without 99.2 %) but not within the *N. thermophila* cluster. The sequence similarity of *N. thermophila* (AB433328) and *N. thermophila* strain A was 99.6% with and without homopolymer regions.

Taken together, divergence and / or number of 18S rRNA gene copies vary between different *Nuclearia* species. Regarding their mutation rates, homopolymer regions can differ drastically from the rest of the sequence. And finally, accumulations of mutations in these regions seem to be species-specific.

Associations of *Nuclearia* spp. with prokaryotes

In total eight of our 17 isolates were associated with endo- and / or ectosymbiotic bacteria. Symbionts could be detected for all *N. delicatula* strains but not for *Nuclearia* isolates from three other clusters (Fig. 1A). Beside these homogeneous branches, also mixed groups were found. In the *N. thermophila* cluster three out of five representatives had symbionts (Fig. 1A).

362 The *N. pattersoni* cluster was also heterogeneous. It was only reported for *N. pattersoni*
363 (Dykova *et al.* 2003) that this amoeba harboured a rickettsial endosymbiont.
364 The non-systematic appearance of symbiotic associations inside the genus *Nuclearia*
365 indicates a species-dependent disposition. As far as we know such a high variability within a
366 single genus has been described only for *Acanthamoeba* spp. (Fritsche *et al.* 1993; Horn *et al.*
367 1999; Horn 2008). Either some *Nuclearia* species evolved traits by which the probability to
368 enter a symbiotic relationship increases or it is a plesiomorph character that has been partly
369 lost. Considering their phylogenetic position within opisthokonts it is of interest to search
370 specifically for such traits in future genetic analysis. Probably, nucleariids have already
371 specific genes and machineries which are involved in selecting and controlling of symbiotic
372 partners (Bosch 2014). The question about the frequency of prokaryotic symbionts in
373 unicellular opisthokonts in general still remains to be addressed. Today it is not clear if the
374 lack of knowledge simply derives from the low number of studies especially looking for
375 symbiotic associations or if the highly diverse interactions inside the genus *Nuclearia* are an
376 exceptional phenomenon.
377
378 **_N. thermophila_ isolates and their ectosymbionts**
379 In a previous study (Dirren *et al.* 2014) we identified the ectosymbiont of *N. thermophila*
380 strain N as the betaproteobacterium *Paucibacter toxinivorans* (Rapala *et al.* 2005) and
381 designed the specific CARD-FISH probe 'Pauci995' (Table 2). Within the *N. thermophila*
382 cluster, only strain A of our new isolates was also associated with ectosymbiotic bacteria right
383 after isolation (Fig. 2A). Unfortunately during cultivation, these bacteria got lost (Figs. 2B)
384 before CARD-FISH filters could be prepared. Although cells were surrounded by a
385 glycocalyx, no ectosymbionts were observed for strain D6 (Fig. 2C; Supplementary Fig. S1C)
386 and strain B1 (Fig. 2D). Since the ectosymbiont of strain N (*P. toxinivorans* strain SD41) was
387 available as pure culture, we checked if the other strains could be infected with these bacteria.

When we added an aliquot (1 ml) of a pure bacterial culture to the medium of ectosymbiont-free isolates, we observed a colonisation of strains A and D6 (Fig. 3A-D). Surprisingly, this was not the case for strain B1. This experiment indicated a highly specific interaction of *P. toxinivorans* strain SD41 with only one phylotype of the *N. thermophila* cluster (strain D6, A and N; see Fig. 1A). The fact that the ectosymbiont did not colonise the glycocalyx of the close relative strain B1 points to a distinct contribution of the host to this symbiosis.

The importance of a glycocalyx has been most extensively investigated for epithelial cells of the gastrointestinal tract (Moran *et al.* 2011). The composition of glycoproteins produced by the host determines the physical (e.g. viscosity) and chemical (e.g. site for bacterial adhesion) nature of this extracellular structure and thus the interaction with bacteria. On the other hand, the composition of the glycocalyx can be modulated by bacteria in distinct ways (Hooper and Gordon 2001). This suggests a cross-talk between host and bacteria mediated by the glycocalyx. Furthermore, in the early branching metazoan *Hydra*, receptors, species-specific antimicrobial peptides (Bosch 2014) and even viruses (Bosch *et al.* 2015) have been shown to be main factors shaping the ectosymbiotic bacterial community. Unfortunately, the molecular interactions between the *N. thermophila* strains and *P. toxinivorans* are yet not studied.

N. thermophila isolates and their endosymbionts

In the *N. thermophila* cluster three (A, D6 and N) out of four isolates harboured the gammaproteobacterial endosymbiont *Ca.* Endonucleariobacter rarus (Fig. 4A-H and Dirren *et al.* (2014)). Hybridisation with the specific probe CoNuc67 (Table 2) resulted in positive signals from all bacteria in strains A and D6 (Fig. 4C, 4G-H). In contrast, endosymbionts were missing in strain B1 (Fig. 3E-F) which additionally had a slightly divergent 18S rRNA gene sequence (Fig. 1A).

413 Interestingly, 18S rRNA gene sequences of strains D6, A and N were identical, but 16S rRNA
414 gene sequences of their endosymbiont *Ca.* Endonucleariobacter rarus were slightly different.
415 Endosymbionts of strains D and A formed a sister group to bacteria of strain N (Fig. 5A),
416 although strains A and N were isolated from the same lake, and strain D6 from a 25 km
417 distant lake.
418
419 **_N. delicatula_ isolates and their ectosymbionts**
420 Four of our *N. delicatula* strains (D, G, S4 and D4) had both ecto- and endosymbionts (Figs.
421 2E-I, 3I-P, 4I-T). Strain B6 was only associated with ectosymbionts (Figs. 2J, 3G-H). Based
422 on the 16S rRNA gene clone library of strain G (Supplementary Fig. S3A) three specific
423 oligonucleotide probes were designed: Bu154, Le827 and Del1424 (Table 2). Ectosymbionts
424 of strain G could be hybridised with the betaproteobacterial probe Bu154 (Fig. 4Q-T). The
425 closest described relative (98.6 % sequence similarity) to the cluster covered by this probe
426 was *Inhella inkyongensis* (Song *et al.* 2009). Phylogeny of nucleariid's ectosymbionts (Fig.
427 5B) highlights that these ectosymbiotic bacteria are related (95.5 % sequence similarity) to the
428 earlier identified ectosymbiont of *N. thermophila* strain N (*P. toxinivorans*). *Inhella* sp. and *P.*
429 *toxinivorans* have both sequence divergences to the bacteriochlorophyll *a*-containing bacteria
430 *Roseateles* (Suyama *et al.* 1999) and *Rubrivivax* (Willems *et al.* 1991) of ~4 and ~5 %,
431 respectively. They form a metabolically diverse group sometimes referred to as 'Sphaerotilus-
432 Leptothrix group' (Spring 2006; Song *et al.* 2009) inside the family Comamonadaceae. As far
433 as we know, a symbiotic live style has not been reported for any representative of this group.
434 Nucleariid amoebae are conspicuous concerning their nutrition: They can feed on harmful
435 filamentous cyanobacteria, without being affected by toxic secondary metabolites (Dirren *et*
436 *al.* 2014). In the previous study we showed that *P. toxinivorans* was able to degrade
437 microcystins, the cyanobacterial toxins stored in food organisms. In the case of *Inhella* sp. we

438 have yet no proof for any similar metabolic capability. However, the spatial proximity to the
439 host's cell surface suggests an exchange of metabolites between the symbiotic partners.
440
441 ***N. delicatula* isolates and their endosymbionts**
442 The gammaproteobacterial probes Le827 and the deltaproteobacterial probe Del1424 gave
443 positive CARD-FISH signals for intracellular bacteria of *N. delicatula* strain G and no signals
444 from bacteria in the cultivation medium. Endosymbionts hybridised with probe Le827
445 specific for a cluster of gammaproteobacteria were evenly distributed and represented a small
446 part of total bacteria inside the cells (Figs. 3I-J, 4P). Due to the homogenous distribution and
447 their estimated abundance by CARD-FISH, we could assign this phylotype to distinct
448 morphological features (morphotype 1) observed on TEM pictures (Fig. 6A-B). Bacteria had
449 two membranes of a typical gram-negative cell wall and an electron dense spot inside cells
450 (Fig. 6C-D). They were localized in the cytoplasm and mostly surrounded by an electron
451 translucent halo but never by an additional membrane. Some intracellular bacteria observed in
452 *N. radians* display remarkable morphological similarities to bacteria in *N. delicatula* strain G
453 (see Plate 4c from Cann and Page (1979)). No described relatives of our endosymbiotic
454 bacteria could be found in public databases. Apart from some sequences of uncultured
455 gammaproteobacteria (highest sequence similarity 94.3 %), the closest relatives were
456 *Candidatus* Berkiella aquae (88.5 % sequence similarity) and *Candidatus* Berkiella
457 cookevillensis (88.1 % sequence similarity) (Fig. 5C). These bacteria (Mehari *et al.* 2015)
458 were found after infection inside the nucleus of *Acanthameoba polyphaga*. We never detected
459 bacteria inside the nuclear membrane of strain G and endosymbionts differed morphologically
460 from the recently characterised symbionts (Mehari *et al.* 2015, e.g. no electron dense spot).
461 The 16S rRNA gene sequences of these symbiotic bacteria and strain G's endosymbiont are
462 too much diverged to resolve their phylogenetic relationship based solely on this marker gene.
463 Thus corresponding branches had to be collapsed (low support values) in the phylogenetic

464 tree (Fig. 5C). We propose the taxonomic status "*Candidatus* Ovatusbacter abovo" for the
465 endosymbiont of *N. delicatula* strain G.
466 Double-hybridisation with the gammaproteobacterial probe Le827 and the
467 deltaproteobacterial probe Del1424 showed different endosymbionts in strain G being
468 hybridised (Fig. 4P). In contrast to the even distribution and low frequency of bacteria
469 labelled with Le827, endosymbionts hybridized with Del1424 showed a lumped occurrence
470 and were highly abundant (Figs. 3K-L, 4P). These characteristics corresponded to the other
471 prominent morphological phenotype (morphotype 2) seen on TEM pictures (Fig. 6A-B). Cells
472 had again a typical gram-negative cell wall structure (Fig. 6E-F) but in contrast to
473 "*Candidatus* Ovatusbacter abovo" they were always surrounded by an additional host derived
474 membrane. Small vacuole-like structures harboured single cells (Fig. 6G-H) or multiple
475 bacteria of morphotype 2 (Fig. 6E-F). We even detected these endosymbionts inside food
476 vacuoles, often attached to the membrane of the vacuole, together with remnants of the food
477 organism *P. rubescens* (Fig. 6B, G-H). In contrast to cyanobacterial cells, endosymbiotic
478 bacteria seemed to be resistant to digestion. This observation in combination with the fact that
479 the deltaproteobacterial probe Del1424 did not hybridise with bacteria in the cultivation
480 medium speaks against a possible role of these intracellular bacteria as food.
481 Usually bacterial pathogens are taken up by phagocytosis and then either prevent the fusion of
482 lysosomes (e.g. *Legionella pneumophila*; Roy and Kagan 2000) or escape the phagosomes
483 (e.g. *Rickettsia prowazekii*; Whitworth *et al.* 2005). Due to the facts that cyanobacterial cells
484 were digested in food vacuoles and endosymbionts were never seen freely in the cytoplasm,
485 there is no indication for any of these two strategies. TEM pictures of *Acanthamoeba*
486 *castellanii* infected with the pathogenic symbiont '*Candidatus* Jidaibacter acanthamoeba'
487 (Fig. 1 in Schulz *et al.* (2015)) resemble conspicuously our observations of the frequent
488 endosymbiont. In contrast to this accordance, types of the symbioses seem to differ. The
489 regular exponential growth of the host *N. delicatula* speaks against a severe pathogenic nature

of its endosymbiotic bacteria. Again, no close relatives of this endosymbiont belonging to the deltaproteobacteria were found in public data bases. The closest relative (89.8 % sequence similarity) was a pathogenic bacterium of daphnids named *Spirobacillus cienkowskii* (Rodrigues *et al.* 2008). None of the sequences included in the phylogenetic tree (Fig. 5C) clustered together with this endosymbiont of strain G. Thus, we propose the taxonomic status "*Candidatus* Turbabacter delicatus" for these bacteria. Specific hybridisation with the deltaproteobacterial probe Del1424 showed that the endosymbiont was also present in cells of strains S4 and D4 (Fig. 3M-P). Like in strain G not all of the intracellular bacteria were labelled. In contrast to the positive hybridisation with the gammaproteobacterial probe Le827 with the other part of endosymbionts in strain G, no signal was obtained for strains S4 and D4. Most probably these strains additionally harboured other so far unidentified endosymbiotic bacteria.

The specific alphaproteobacterial probe AlRick85 was designed based on a cluster of sequences in the 16S rRNA gene clone library of *N. delicatula* strain D (Supplementary Fig. S3B). AlRick85 hybridised specifically with all endosymbiotic bacteria of this isolate (Fig. 4I-L). In public databases no closely related sequences were found except for some uncultured bacteria. The closest characterised relatives were *Candidatus* Finniella inopinata (89.1 % sequence similarity) and *Candidatus* Finniella lucida (88.4 % sequence similarity) which are rickettsial endosymbionts of viridiraptorid amoeboflagellates (Fig. 5C). Sequences of the alphaproteobacterial endosymbiont of strain D affiliated with the recently established family *Candidatus* Paracaedibacteraceae (Hess *et al.* 2016). This family is formed by endosymbionts of different protists. So far they were found in Rhizaria, Excavata and Amoebozoa. Here we report for the first time a representative of this family inside an opisthokont protist. TEM pictures proved that only one bacterial morphotype was found in the cytoplasm (Fig. 7A): gram-negative bacterial cells with invaginated cell wall which were surrounded by an electron translucent halo (Fig. 7B-C). No additional host derived membrane

or electron-dense layer (which was observed for the endosymbionts of the viridiraptorid amoeboflagellates) were detected for this endosymbiont. The observed features were consistent with the descriptions for the members of the family *Candidatus* Paracaedibacteraceae. Due to a distinct phylogenetic clustering, several morphological differences and a new host habitat, we propose the provisional name "*Candidatus* Intestinusbacter nucleariae" for these endosymbiotic bacteria.

Description of "*Candidatus* Ovatusbacter abovo" (Gammaproteobacteria)

Etymology: L. masc. adj. *ovatus*, egg-shaped; N.L. masc. n. *bacter*, a rod; N.L. masc. n. *Ovatusbacter*, egg-shaped bacterium, inspired by the appearance on cross-sections (TEM), when cells looked like fried eggs. L. prefix. *ab*, from; L. nt. dat. sing. n. *ovo* of *ovum*, egg; L. *abovo* (*ab ovo*) mythological allusion to one of the two eggs of Leda which was the primary cause of the Trojan War; expression used to indicate an ancient origin.

Rod-shaped bacterium up to 1 µm in length (mean length: 0.65 µm and mean width: 0.34 µm; n = 30) with a typical gram-negative cell wall structure and a characteristic central electron-dense spot observed by TEM. Basis of assignment: 16S rRNA gene sequence (accession number: LN875061) and positive signal with the specific CARD-FISH probe Le827 (5'-CCCTAAGGCTTCCAACAGCC -3'). So far only detected in the cytoplasm of *N. delicatula* strain G (accession number: LN875119), isolated from Lake Zurich, Switzerland. Typically 50 – 200 cells could be observed inside this nucleariid host. Uncultured so far.

Description of "*Candidatus* Turbabacter delicatus" (Deltaproteobacteria)

Etymology: L. fem. n. *turba*, noisiness, swarm, mass; N.L. masc. n. *bacter*, a rod; N.L. masc. n. *Turbabacter,* rod-shaped bacterium appearing in masses. L. masc. adj. *delicatus*, spoilt, delicate, referring to the host species *N. delicatula* and to its lifestyle in a protected nutrient-rich niche.

Rod-shaped gram-negative bacterium up to 1.69 µm in length (mean length: 1 µm and mean width: 0.48 µm; n = 30). Cells are found inside vacuole-like structures and food vacuoles (often attached to the membrane) but never freely in the cytoplasm. Bases of assignment: 16S rRNA gene sequence (accession number: LN875050) and positive signal with the specific CARD-FISH probe Del1424 (5'- GCTCACGCGCTTCTGGCTTATAC -3'). Up to now detected in three different *N. delicatula* isolates: strain G, strain S4 and strain D4 (accession numbers: LN875119, LN875117 and LN875116). Usually several hundreds of individuals were observed inside the host species which were isolated from two Swiss Lakes: Lake Zurich and Lake Sempach. Uncultured so far.

Description of "*Candidatus* Intestinusbacter nucleariae" (Rickettsiales Alphaproteobacteria)

Etymology: L. masc. adj. *intestinus*, internal; N.L. masc. n. *bacter*, a rod; N.L. masc. n. *Intestinusbacter*, rod-shaped bacterium living internal (inside eukaryotic cells). N.L. fem. gen. sing. n. *nucleariae* from *Nuclearia*, taxonomic name of the single genus *Nuclearia* within the family Nucleariidae, indicating the affiliation of the host.

Rod-shaped bacterium up to 1.1 µm in length (mean length: 0.71 µm and mean width: 0.29 µm; n = 18) with gram-negative invaginated cell wall organisation and translucent halo (on conventional TEM pictures). Basis of assignment: 16S rRNA gene sequence (accession number: LN875069) and positive signal with the specific CARD-FISH probe AlRick85 (5'-CGTCTGCCACTAACATATGTGAGCT -3'). So far only detected in the cytoplasm of *N. delicatula* strain D (accession number: LN875118), isolated from Lake Zurich, Switzerland. Uncultured so far.

Funding

This study was financed by the Swiss National Fund (SNF 31003A_138473 and SNF 31003A_159842).

Acknowledgements

We thank Jakob Pernthaler (University of Zurich), Gianna Pitsch (University of Zurich) and Sebastian Hess (Dalhousie University) for fruitful discussions and Marvin Moosmann for the help with the isolation of amoebae. TEM imaging was performed with equipment and support of the Centre for Microscopy, University of Zurich.

The authors declared no conflicts of interest.

References

Artari A**.** Morphologische und biologische Studien über *Nuclearia delicatula* Cienk. *Zool Anz* 1889;**12**:408-16

Alegado RA, King N. Bacterial influences on animal origins. *Cold Spring Harb Perspect Biol* 2014, DOI: 10.1101/cshperspect.a016162.

Ashelford KE, Chuzhanova NA, Fry JC, et al. At least 1 in 20 16S rRNA sequence records currently held in public repositories is estimated to contain substantial anomalies. *Appl Environ Microbiol* 2005;**71**:7724-36.

Bosch TC. Rethinking the role of immunity: lessons from *Hydra*. *Trends Immunol* 2014;**35**:495-502.

Bosch TC, Grasis J, Lachnit T. Microbial ecology in *Hydra*: Why viruses matter. *J Microbiol* 2015;**53**:193-200.

Buckley DH, Schmidt TM. Environmental factors influencing the distribution of rRNA from Verrucomicrobia in soil. *FEMS Microbiol Ecol* 2001;**35**:105-12.

Cann JP. The feeding behavior and structure of *Nuclearia delicatula* (Filosea: Aconchulinida). *J Protozool* 1986;**33**:392-6.

Cann JP, Page FC. *Nucleosphaerium tuckeri* nov. gen. nov. sp.- A new freshwater filose amoeba without motile form in a new family Nucleariidae (Filosea: Aconchulinida) feeding by ingestion only. *Arch Protistenk* 1979;**122**:226-40.

Casadevall A. Evolution of intracellular pathogens. *Annu Rev Microbiol* 2008;**62**:19-33.

Daims H, Bruhl A, Amann R, et al. The domain-specific probe EUB338 is insufficient for the detection of all Bacteria: Development and evaluation of a more comprehensive probe set. *Syst Appl Microbiol* 1999;**22**:434-44.

De Rijk P, Neefs J-M, Van De Peer Y, et al. Compilation of small ribosomal subunit RNA sequences. *Nucl Acid Res* 1992;**20**:2075-89.

Dirren S, Salcher MM, Blom JF, et al. Ménage-à-trois: The amoeba *Nuclearia* sp. from Lake Zurich with its ecto- and endosymbiotic bacteria. *Protist* 2014;**165**:745-58.

Dykova I, Veverkova M, Fiala I, et al. *Nuclearia pattersoni* sp. n. (Filosea), a new species of amphizoic amoeba isolated from gills of roach (*Rutilus rutilus*), and its rickettsial endosymbiont. *Folia Parasitol* 2003;**50**:161-70.

Franzenburg S, Walter J, Künzel S, et al. Distinct antimicrobial peptide expression determines host species-specific bacterial associations. *Proc Natl Acad Sci* 2013, DOI: 10.1073/pnas.1304960110.

Fraune S, Anton-Erxleben F, Augustin R, et al. Bacteria-bacteria interactions within the microbiota of the ancestral metazoan *Hydra* contribute to fungal resistance. *ISME J* 2015;**9**:1543-56.

Fraune S, Bosch TC. Long-term maintenance of species-specific bacterial microbiota in the basal metazoan *Hydra*. *Proc Natl Acad Sci* 2007;**104**:13146-51.

Freeman MF, Gurgui C, Helf MJ, et al. Metagenome mining reveals polytheonamides as posttranslationally modified ribosomal peptides. *Science* 2012;**338**:387-90.

Fritsche TR, Gautom RK, Seyedirashti S, et al. Occurrence of bacterial endosymbionts in *Acanthamoeba* spp. isolated from corneal and environmental specimens and contact lenses. *J Clin Microbiol* 1993;**31**:1122-6.

Gast RJ, Sanders RW, Caron DA. Ecological strategies of protists and their symbiotic relationships with prokaryotic microbes. *Trends Microbiol* 2009;**17**:563-9.

Hess S, Suthaus A, Melkonian M. "*Candidatus* Finniella" (Rickettsiales, Alphaproteobacteria), Novel Endosymbionts of Viridiraptorid Amoeboflagellates (Cercozoa, Rhizaria). *Appl Environ Microbiol* 2016;**82**:659-70.

Hooper LV, Gordon JI. Glycans as legislators of host–microbial interactions: spanning the spectrum from symbiosis to pathogenicity. *Glycobiology* 2001;**11**:1R-10R.

Horn M. Chlamydiae as symbionts in eukaryotes. *Annu Rev Microbiol* 2008;**62**:113-31.

Horn M, Fritsche TR, Gautom RK, et al. Novel bacterial endosymbionts of *Acanthamoeba* spp. related to the *Paramecium caudatum* symbiont *Caedibacter caryophilus*. *Environ Microbiol* 1999;**1**:357-67.

Huttenhower C, Gevers D, Knight R, et al. Structure, function and diversity of the healthy human microbiome. *Nature* 2012;**486**:207-14.

Katoh K, Standley DM. MAFFT multiple sequence alignment software version 7: improvements in performance and usability. *Mol Biol Evol* 2013;**30**:772-80.

635 Kiers ET, West SA. Evolving new organisms via symbiosis. *Science* 2015;**348**:392-4.
636 Kikuchi Y, Hayatsu M, Hosokawa T, et al. Symbiont-mediated insecticide resistance. *Proc Natl Acad*
637 *Sci* 2012;**109**:8618-22.
638 Lema KA, Bourne DG, Willis BL. Onset and establishment of diazotrophs and other bacterial
639 associates in the early life history stages of the coral *Acropora millepora*. *Mol Ecol*
640 2014;**23**:4682-95.
641 Levinson G, Gutman GA. Slipped-strand mispairing: a major mechanism for DNA sequence
642 evolution. *Mol Biol Evol* 1987;**4**:203-21.
643 Liu Y, Steenkamp ET, Brinkmann H, et al. Phylogenomic analyses predict sistergroup relationship of
644 nucleariids and Fungi and paraphyly of zygomycetes with significant support. *BMC Evol Biol*
645 2009;**9**:Article No.: 272.
646 Lozupone CA, Stombaugh JI, Gordon JI, et al. Diversity, stability and resilience of the human gut
647 microbiota. *Nature* 2012;**489**:220-30.
648 Ludwig W, Strunk O, Westram R, et al. ARB: a software environment for sequence data. *Nucl Acid*
649 *Res* 2004;**32**:1363-71.
650 Manz W, Amann R, Ludwig W, et al. Application of a suite of 16S rRNA-specific oligonucleotide
651 probes designed to investigate bacteria of the phylum cytophaga-flavobacter-bacteroides in the
652 natural environment. *Microbiol-Uk* 1996;**142**:1097-106.
653 Manz W, Amann R, Ludwig W, et al. Phylogenetic oligodeoxynucleotide probes for the major
654 subclasses of proteobacteria: problems and solutions. *Syst Appl Microbiol* 1992;**15**:593-600.
655 McFall-Ngai M, Hadfield MG, Bosch TC, et al. Animals in a bacterial world, a new imperative for the
656 life sciences. *Proc Natl Acad Sci USA* 2013;**110**:3229-36.
657 Mehari YT, Hayes BJ, Redding KS, et al. Description of '*Candidatus* Berkiella aquae' and '*Candidatus*
658 Berkiella cookevillensis', two intranuclear bacteria of freshwater amoebae. *Int J Syst Evol*
659 *Microbiol* 2015.
660 Moon-van der Staay SY, De Wachter R, Vaulot D. Oceanic 18S rDNA sequences from picoplankton
661 reveal unsuspected eukaryotic diversity. *Nature* 2001;**409**:607-10.
662 Moran AP, Gupta A, Joshi L. Sweet-talk: role of host glycosylation in bacterial pathogenesis of the
663 gastrointestinal tract. *Gut* 2011;**60**:1412-25.
664 Muyzer G, Ramsing NB. Molecular methods to study the organization of microbial communities.
665 *Water Sci Technol* 1995;**32**:1-9.
666 Nakayama T, Marin B, Kranz HD, et al. The basal position of scaly green flagellates among the green
667 algae (Chlorophyta) is revealed by analyses of nuclear-encoded SSU rRNA sequences. *Protist*
668 1998;**149**:367-80.
669 Neef A. *Anwendung der In-situ-Einzelzell-Identifizierung von Bakterien zur Populationsanalyse in*
670 *komplexen mikrobiellen Biozönosen*. PhD Thesis, Technische Universität München
671 Ouwerkerk JP, de Vos WM, Belzer C. Glycobiome: Bacteria and mucus at the epithelial interface.
672 *Best Pract Res Cl Ga* 2013;**27**:25-38.
673 Paracer S, Ahmadjian V. *Symbiosis: An introduction to biological associations*. New York: Oxford
674 University Press, 2000.
675 Patterson DJ. The genus *Nuclearia* (Sarcodina, Filosea): Species composition and characteristics of
676 the taxa. *Arch Protistenk* 1984;**128**:127-39.
677 Pernin P. Study in vivo of an ameoba with pseudopodes filosa: *Nuclearia simplex* Cienkowski 1865
678 (Protozoa, Rhizopodea, Filosia, Aconchulinida). *Protistologica* 1976;**12**:555-62.
679 Pruesse E, Quast C, Knittel K, et al. SILVA: a comprehensive online resource for quality checked and
680 aligned ribosomal RNA sequence data compatible with ARB. *Nucl Acid Res* 2007;**35**:7188-96.
681 Rapala J, Berg KA, Lyra C, et al. *Paucibacter toxinivorans* gen. nov., sp nov., a bacterium that
682 degrades cyclic cyanobacterial hepatotoxins microcystins and nodularin. *Int J Syst Evol Microbiol*
683 2005;**55**:1563-8.
684 Rodrigues JLM, Duffy MA, Tessier AJ, et al. Phylogenetic characterization and prevalence of
685 "*Spirobacillus cienkowskii*," a red-pigmented, spiral-shaped bacterial pathogen of freshwater
686 *Daphnia* species. *Appl Environ Microbiol* 2008;**74**:1575-82.
687 Rodríguez-Ezpeleta N, Brinkmann H, Burey SC, et al. Monophyly of primary photosynthetic
688 eukaryotes: green plants, red algae, and glaucophytes. *Curr Biol* 2005;**15**:1325-30.
689 Roller C, Wagner M, Amann R, et al. *In situ* probing of gram-positive bacteria with high DNA G + C
690 content using 23S rRNA targeted oligonucleotides. *Microbiol-Uk* 1994;**140**:2849-58.

691 Roy CR, Kagan JC. *Evasion of phagosome lysosome fusion and establishment of a replicative*
692 *organelle by the intracellular pathogen Legionella pneumophila*. Austin: Landes Bioscience,
693 2000.
694 Schulz F, Martijn J, Wascher F, et al. A rickettsiales symbiont of amoebae with ancient features.
695 *Environ Microbiol* 2015, DOI: 10.1111/1462-2920.12881.
696 Smith JM. Generating novelty by symbiosis. *Nature* 1989;**341**:284-5.
697 Song J, Oh HM, Lee JS, et al. *Inhella inkyongensis* gen. nov., sp. nov., a new freshwater bacterium in
698 the order Burkholderiales. *J Microbiol Biotechn* 2009;**19**:5-10.
699 Spring S. The genera Leptothrix and Sphaerotilus. In: Dworkin M, Falkow S, Rosenberg E, et al.
700 (eds.) *The Prokaryotes*. New York: Springer, 2006, 758-77.
701 Stamatakis A, Hoover P, Rougemont J. A rapid bootstrap algorithm for the RAxML web servers. *Syst*
702 *Biol* 2008;**57**:758-71.
703 Steenkamp ET, Wright J, Baldauf SL. The protistan origins of animals and fungi. *Mol Biol Evol*
704 2006;**23**:93-106.
705 Suyama T, Shigematsu T, Takaichi S, et al. *Roseateles depolymerans* gen. nov., sp. nov., a new
706 bacteriochlorophyll a-containing obligate aerobe belonging to the beta-subclass of the
707 Proteobacteria. *Int J Syst Bacteriol* 1999;**49**:449-57.
708 Thrash JC, Boyd A, Huggett MJ, et al. Phylogenomic evidence for a common ancestor of
709 mitochondria and the SAR11 clade. *Sci Rep* 2011, DOI: 10.1038/srep00013.
710 Wallner G, Amann R, Beisker W. Optimizing fluorescent *in situ* hybridization with rRNA-targeted
711 oligonucleotide probes for flow cytometric identification of microorganisms. *Cytometry*
712 1993;**14**:136-43.
713 Walsby AE, Avery A, Schanz F. The critical pressures of gas vesicles in *Planktorhrix rubescens* in
714 relation tothe depth of winter mixing in Lake Zurich, Switzerland. *J Plankton Res* 1998;**20**:1357-
715 75.
716 Whitworth T, Popov VL, Yu X-J, et al. Expression of the *Rickettsia prowazekii pld* or *tlyC* gene in
717 *Salmonella enterica* serovar typhimurium mediates phagosomal escape. *Infect Immun*
718 2005;**73**:6668-73.
719 Willems A, Gillis M, De Ley J. Transfer of *Rhodocyclus gelatinosus* to *Rubrivivax gelatinosus* gen.
720 nov., comb. nov., and phylogenetic relationships with *Leptothrix*, *Sphaerotilus natans*,
721 *Pseudomonas saccharophila*, and *Alcaligenes latus*. *Int J Syst Evol Microbiol* 1991;**41**:65-73.
722 Wylezich C, Karpov SA, Mylnikov AP, et al. Ecologically relevant choanoflagellates collected from
723 hypoxic water masses of the Baltic Sea have untypical mitochondrial cristae. *BMC Microbiol*
724 2012;**12**:1-13.
725 Yilmaz LS, Parnerkar S, Noguera DR. mathFISH, a web tool that uses thermodynamics-based
726 mathematical models for *in silico* evaluation of oligonucleotide probes for fluorescence *in situ*
727 hybridization. *Appl Environ Microbiol* 2011;**77**:1118-22.
728 Yoshida M, Nakayama T, Inouye I. *Nuclearia thermophila* sp. nov. (Nucleariidae), a new nucleariid
729 species isolated from Yunoko Lake in Nikko (Japan). *Europ J Protistol* 2009;**45**:147-55.
730 Zettler LAA, Nerad TA, O'Kelly CJ, et al. The nucleariid amoebae: More protists at the animal-fungal
731 boundary. *J Eukaryot Microbiol* 2001;**48**:293-7.

732

Figure 1

Phylogenetic analysis of the *Nuclearia* spp. isolates. (A) 18S rRNA gene based Maximum Likelihood (ML) tree with posterior probabilities from Bayesian interference (BI); ML Bootstrap value / BI probability. Described *Nuclearia* species are shown in bold and *Candida* was used as outgroup. Hypothetical gain (curved arrow) and loss (bar) of features 'cyst production' (Cysts) and 'formation of syncytia' (Syncytia) are shown. Detected ectosymbionts (EC) and endosymbionts (EN) are indicated with a filled square for the respective isolate. Scale bar: number of nucleotide substitutions per site. (B) Cladistic tree based on morphological characters of the *Nuclearia* spp. isolates. X-axis: similarity value (Jaccard coefficient). The affiliation of amoeboid isolates to described species are indicated on the right hand. Isolates with associated symbionts are grey shaded.

Figure 2

Light microscopical images of 12 *Nuclearia* spp. isolates. (A) Nucleariid cell attached to a *P. rubescens* filament surrounded by ectosymbiotic bacteria right after isolation. (B) Feeding individual after loss of ectosymbionts (three months later). (C) Vegetative cell (left) and cyst (right) next to each other. (D) Elongated organism with phagocytised *P. rubescens* fragments. (E) Green cell (due to partly digested pigments of food organisms) colonised by ectosymbiotic bacteria 9 months after isolation. (F) Amoeboid multinucleated organism which lost ectosymbionts (three years later). (G) Multinucleate spherical individual with symbiotic bacteria inside the glycocalyx. (H) Nearly spherical cell with radiating filopodia. Note food vacuoles and two nucleoli. (I) Feeding individual with a large food vacuole containing remnants of *P. rubescens* filaments at different states of digestion. Ectosymbiotic bacteria surround the multinucleate cell. (J) Organism partly attached to the surface colonised by symbiotic bacteria. Concentrated filopodia indicate the direction of locomotion. (K) Amoeboid cell with a prominent nucleolus. (L) Individual with ingested fragments of *P.*

rubescens. (M) Spherical cell freely floating. (N) Amoeboid organism moving on surface. All pictures were taken with Differential Interference Contrast (DIC) and scale bars indicate 20 µm.

Figure 3

CARD-FISH of bacterial symbionts associated with (A-F) *N. thermophila* and (G-P) *N. delicatula* isolates. For abbreviations of applied oligonucleotide probes see Table 2. Different fluorophore-specific filter sets were used to image the cells after hybridisation. The first two and the last two columns of each row represent always the same cell. (A) Cell with ingested *P. rubescens* filaments and accompanying bacteria after DAPI staining. (B) Ectosymbiotic bacteria hybridised with the probe Pauci995. (C) Cell with well-preserved glycocalyx. Ectosymbionts are still arranged close to the cell surface. (D) The probe Pauci995 hybridised with ectosymbionts. (E) The nucleariid cell stained with DAPI. (F) No endosymbionts detected with the probe EUBI-III. (G) Three nuclei and ectosymbionts observed after DAPI staining. (H) No endosymbionts were detected with the probe EUBI-III. (I) Nuclei, endosymbionts and ingested *P. rubescens* filaments after DAPI staining. (J) Merged picture of the CARD-FISH signal and the autofluorescence. A small part of the endosymbionts are hybridised with the probe Le827. (K) Individual with three nuclei, endo- and ectosymbiotic bacteria after DAPI staining. (L) Merged picture of the CARD-FISH signal and the autofluorescence. The main part of endosymbionts hybridised with the probe Del1424. (M) Nucleariid cell with three nuclei and endosymbionts attached to a *P. rubescens* filament. (N) Merged picture of the CARD-FISH and the DAPI signal. One part of the endosymbiotic bacteria is hybridised with the probe Del1424. (O) Individual with three nuclei, endosymbionts and accompanying bacteria after DAPI staining. (P) Merged picture of the CARD-FISH and the DAPI signal. The mayor part of endosymbionts are hybridised with the probe Del1424. Scale bars represent 20 µm.

Figure 4

CARD-FISH preparations of (A-H) *N. thermophila* and (I-T) *N. delicatula* isolates embedded in (A-P) gelatine and (Q-T) agarose. Single nucleariid cells of different isolates are shown after hybridisation. For abbreviations of applied oligonucleotide probes see Table 2. Always the same cell is depicted in one row. Light microscopical pictures are placed in the first column, further columns represent epifluorescence images taken with fluorophore-specific filter sets. Pictures (Q-T) were recorded with a confocal laser scanning microscope. (A) Nucleariid cell next to a *P. rubescens* filament. (B) Endosymbiotic and accompanying bacteria after DAPI staining. (C) All endosymbionts hybridised with the probe CoNuc67. (D) Strong autofluorescence of the phototrophic cyanobacterium *P. rubescens*. (E) Cell with radiating filopodia. (F) Nucleus and bacteria stained with DAPI. (G) Hybridisation of all endosymbionts with the probe CoNuc67. (H) Merged picture of autofluorescence (originating from ingested *P. rubescens*) and the CARD-FISH signal. (I) Nucleariid cell with two nuclei. (J) Endosymbionts visible after DAPI staining. (K) The oligonucleotide probe EUBI-III hybridised with endosymbionts and bacteria in the cultivation medium. (L) All endosymbionts hybridised specifically with the probe AlRick85. (M) Spherical cell with radiating filopodia. (N) Three nuclei and bacterial endosymbionts stained with DAPI. (O) Merged picture of autofluorescence (*P. rubescens* in food vacuoles) and DAPI. (P) Double hybridisation with the two probes Le827 (few scattered bacteria) and Del1424 (many bacteria and lumped distribution). (Q) Spherical *Nuclearia* cell embedded in agarose. (R) Bacteria surrounding the cell stained with DAPI. (S) Ectosymbiotic bacteria hybridised with the probe Bu154. (T) Merged pictures of hybridised and DAPI stained organisms. Scale bars represent 20 µm.

Figure 5

Phylogenetic analyses of (A) *Candidatus* Endonucleariobacter rarus, (B) ectosymbionts and (C) endosymbionts based on their 16S rRNA genes. Symbionts of *Nuclearia* spp. are shown in bold. ML trees with posterior probabilities from BI; ML Bootstrap value / BI probability. Branches with bootstrap values ≤ 60 were collapsed. Scale bars: numbers of substitutions per site. Ectothiorhodospiraceae, *Polynucleobacter* and Verrucomicrobia were used as outgroups, respectively.

Figure 6

TEM images of *N. delicatula* strain G. (A and B) Overview of two different nucleariid cells displaying nuclei with their nucleoli (no) and numerous bacteria inside their cytoplasm. Magnifications of squares are shown in C, E and G, respectively. Two morphotypes of endosymbiotic bacteria can be distinguished. The less abundant morphotype 1 can be found freely inside the cytoplasm, whereas the prominent morphotype 2 is present in vacuole-like structures (v). (C) Two bacteria and (D) a dividing individual of morphotype 1 inside the nucleariid cell. A characteristic central electron-dense spot and a typical gram-negative cell wall structure with two membranes (arrowheads) are visible. No peribacterial membrane is present but an electron translucent halo surrounds the cell. (E and F) Cells having the characteristics of morphotype 2 are tightly packed inside a peribacterial membrane (arrow). The gram-negative cell wall organisation with two membranes (arrowheads) is visible. The cell content of this endosymbiont has a homogenous appearance on TEM pictures. (G) In the big central food vacuole (see overview B) an intact *P. rubescens* filament (p) and remnants of digested cyanobacteria can be seen. In addition to the food organism (*P. rubescens*) bacteria of the morphotype 2 are present inside the food vacuoles (v). Many bacteria seem to be attached to the membrane. Additionally single or few cells of this morphotype are enclosed in membranes apparently not connected to the food vacuole. (H) Higher magnification of the

interface between food vacuole and cytoplasm. Bacteria of the morphotype 2 are attached to the membrane sometimes forming cavities. Bacteria seem to be intact and not digested. d, dictyosome; f, filopodium; g, glycocalyx; m, mitochondrion; no, nucleolus; p, *P. rubescens* filament; v, vacuole-like structures. Scale bars represent 10 µm in (A,B), 4 µm in (G), 1 µm in (H), and 500 nm in (C-F).

Figure 7

TEM images of *N. delicatula* strain D. (A) Overview showing the highly vacuolated (v) nucleariid cell with two prominent nucleoli (no) and a filopodium (f). Inside the big central food-vacuole a *P. rubescens* filament (p) and remnants of already digested cyanobacterial cells are visible. Only one morphotype of endosymbionts with homogenous electron-dense cell content is present. (B) Higher magnification of three endosymbionts (square in (A)). Bacteria are located freely in the cytoplasm surrounded by a pronounced electron-translucent halo. (C) Higher magnification of one bacterial cell (square in (B)). No peribacterial membrane but two membranes (arrowheads) of the gram-negative cell wall are visible. d, dictyosome; f, filopodium; m, mitochondrion; no, nucleolus; p, *P. rubescens* filament; v, vacuole-like structures. Scale bars represent 10 µm in (A), 2 µm in (B) and 500 nm in (C).

Table 1: Features of *Nuclearia* isolates. The following features were observed for all strains and thus are not listed: spherical form, flattened form, nucleolus, glycocalyx and branching of filopodia. If not stated otherwise, strains were isolated from benthic samples. Strains are listed according to the phylogenetic tree shown in Fig.1A. In case that bacterial symbionts could be identified with FISH, the adequate oligonucleotide probes are listed (see Table 2 for probes abbreviations). Lake Zurich: 47°19'11.5"N, 8°33'10.1"E, Lake Hallwil: 47°18'16.3"N, 8°13'03.3"E, Lake Sempach: 47°08'15.8"N, 8°08'25.8"E, Lake Baldegg: 47°11'38.9"N, 8°15'46.6"E, Lake Soppi: 47°05'25.6"N, 8°04'51.5"E.

***Nuclearia* sp. Strain**	**Nucleus**	**Ectosymbiont**	**Endosymbiont**	**Cysts**	**Mean size (range); *n* (sizes in µm)**	**18S rRNA sequence**	**Isolation date; Source**
***N. delicatula* strain G**	Multinucleate	Bu154	Del1424 & Le827	-	26 (17.2 - 45.8); *n=100*	LN875119	Oct 2012; Lake Zurich
***N. delicatula* strain D**	Multinucleate	+ (lost)[1]	AlRick85	-	20.4 (10.7 - 82.2); *n=133*	LN875118	Feb 2012; Lake Zurich
***N. delicatula* strain S4**	Multinucleate	+ (lost)[1]	Del1424	-	24.5 (12.8 - 104.8); *n=100*	LN875117	Oct 2014; Lake Sempach
***N. delicatula* strain D4**	Multinucleate	+ (lost)[1]	Del1424	-	24 (13.8 - 42.6); *n=100*	LN875116	Oct 2014; Lake Sempach
***N. delicatula* strain B6**	Multinucleate	+ (lost)[1]	-	-	26.7 (15 - 45.6); *n=107*	LN875115	Sep 2014; Lake Hallwil
***N. moebiusi* strain K**	Uninucleate	-	-	-	9.8 (3.8 - 15.1); *n=100*	LN875108	Oct 2012; Lake Zurich
***N. thermophila* strain B1**	Uninucleate	-	-	+	15.4 (9.5 - 23.2); *n=100*	LN875121/22	Nov 2013; Lake Zurich
***N. thermophila* strain D6**	Uninucleate	-	CoNuc67	+	15.7 (9.4 - 22.7); *n=100*	LN875109	Sep 2014; Lake Hallwil
***N. thermophila* strain A**	Uninucleate & Multinucleate syncytia	+ (lost)[1]	CoNuc67	+	17.7 (9.8 - 28.3); *n=270*	LN875106	May 2011; Lake Zurich
***N. thermophila* strain N**	Uninucleate & Multinucleate syncytia	Pauci995	CoNuc67	+	16.4 (7.2 – 29); *n=448*	HG530253	Aug 2011; Lake Zurich
***Nuclearia* sp. strain B3**	Uninucleate	-	-	-	8.7 (5 - 14.2); *n=100*	LN875120	Sep 2014; Lake Baldegg [2]
***Nuclearia* sp. strain A5**	Uninucleate & Multinucleate syncytia	-	-	-	9.2 (5.4 - 15.4); *n=100*	LN875107	Sep 2014; Lake Hallwil [2]
***N. pattersoni* strain B4**	Uninucleate	-	-	+	8.4 (5.4 - 15.3); *n= 100*	LN875111	Oct 2014; Lake Soppi [2]
***N. pattersoni* strain A2**	Uninucleate	-	-	+	9.9 (6.5 - 17.8); *n=100*	LN875110	Sep 2014; Lake Baldegg [2]
***Nuclearia* sp. strain NZ**	Uninucleate	-	-	-	16.7 (10.6 - 28.4); *n=100*	LN875112	Oct 2012; Lake Zurich [2]
***Nuclearia* sp. strain A1**	Uninucleate	-	-	-	12.3 (8.2 - 18.3); *n=106*	LN875113	Oct 2014; Lake Sempach
***Nuclearia* sp. strain D1**	Uninucleate	-	-	-	11.9 (6.9 - 19.4); *n=124*	LN875114	Oct 2014; Lake Sempach

[1] Amoebae lost bacterial ectosymbionts during long-term cultivation.
[2] Amoebal strains were isolated from the pelagic zone of the respective lake.

Table 2: Specific CARD-FISH probes applied in this study. Affiliation of the target bacteria to major taxonomic groups are given in brackets: AlRick85 (Alphaproteobacteria), Bu154 and Pauci995 (Betaproteobacteria), Del1424 (Deltaproteobacteria), CoNuc67 and Le837 (Gammaproteobacteria).

Probe (Reference)	**Sequence (5' to 3')**	**Specificity**	**FA in %[1]**	**Hits in RDP[2]/ Δ FA in % to the non-targets[3]**
CoNuc67 (Dirren *et al.* 2014)	ATTGCTACACACTCTGTTACCG	"*Candidatus* Endonucleariobacter rarus"	70	0; 2; 31 / 30.5
Pauci995 (Dirren *et al.* 2014)	AATCTCTTCGGGATCTCTGACATG	*Paucibacter toxinivorans*	70	23; 77; 465 / 0
Bu154 (this study)	CGAACAGTTATCCCCCACTACC	*Inhella* sp. ectosymbiont of strain G	55	17; 14859; 29751 / 0
Le837 (this study)	CCCTAAGGCTTCCAACAGCC	"*Candidatus* Ovatusbacter abovo"	60	0; 1; 6 / 33.3
Del1424 (this study)	GCTCACGCGCTTCTGGCTTATAC	"*Candidatus* Turbabacter delicatus"	70	0; 0; 0 / 30.7
AlRick85 (this study)	CGTCTGCCACTAACATATGTGAGCT	"*Candidatus* Intestinusbacter nucleariae"	70	0; 0, 1 / 69.9

[1] Formamide concentrations in the hybridisation buffer.

[2] Number of hits with the 'Probe Match' tool in the RDP database: zero mismatches; one mismatch; two mismatches.

[3] Minimal difference in formamide concentrations between target and non-targets calculated with the 'Mismatch Analysis' tool from mathFISH.

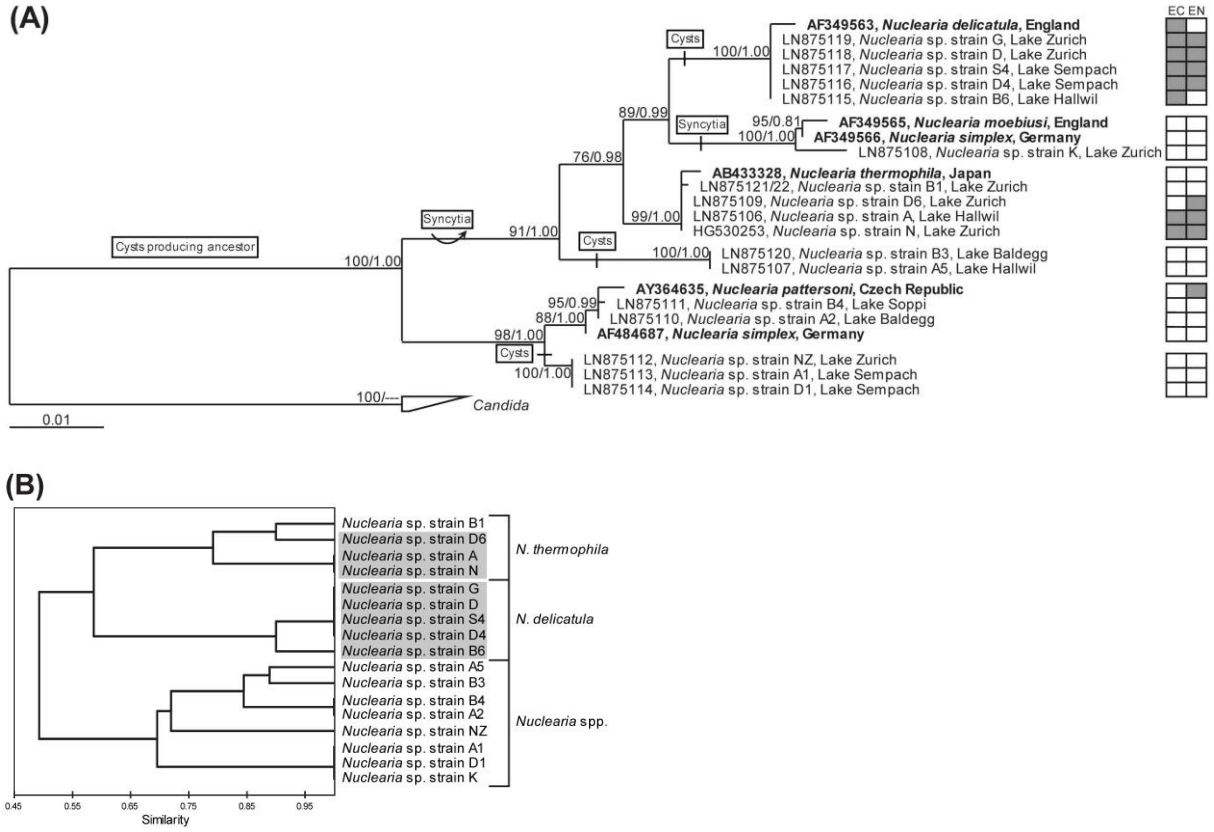

Figure 1 (Dirren & Posch)

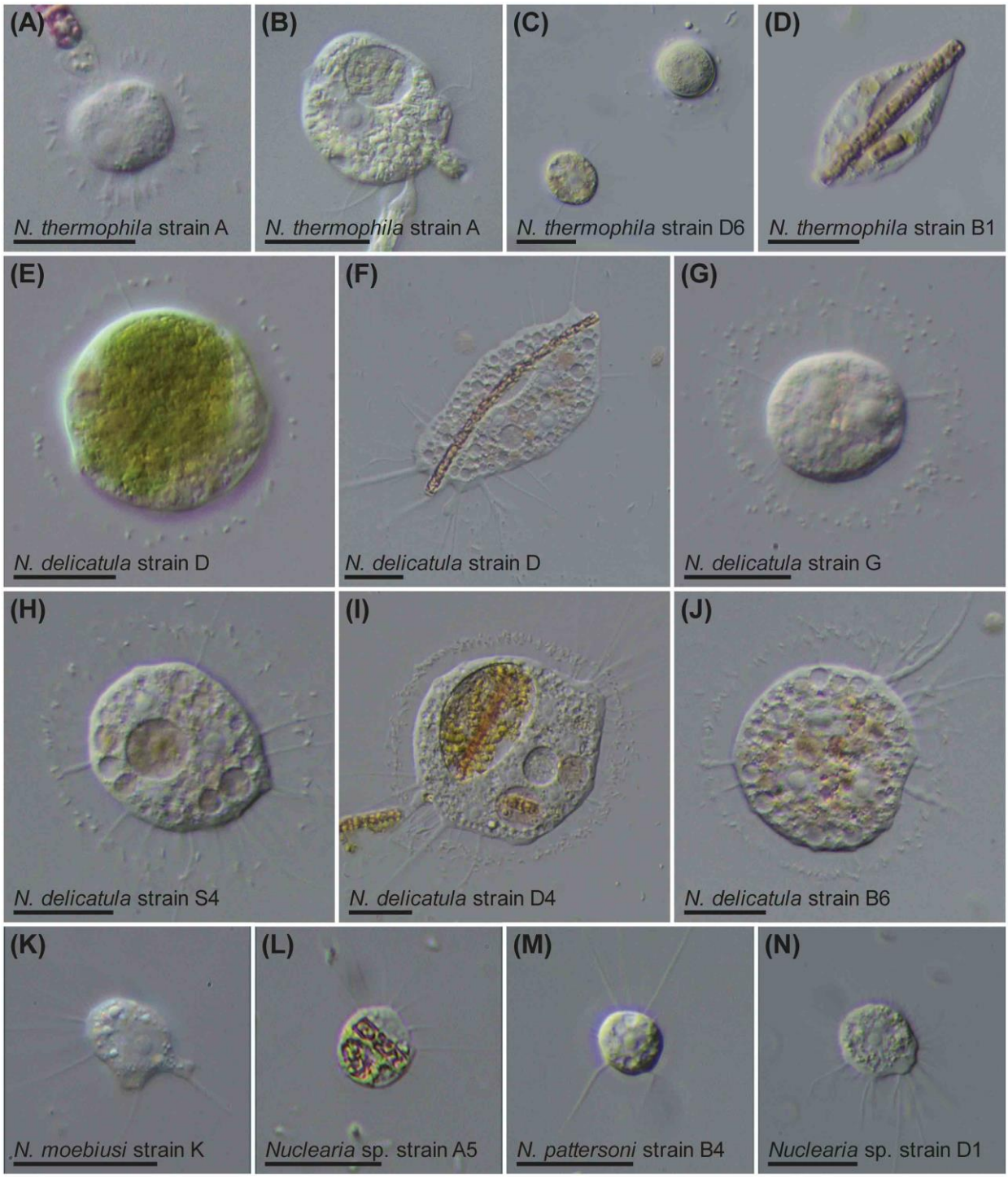

Figure 2 (Dirren & Posch)

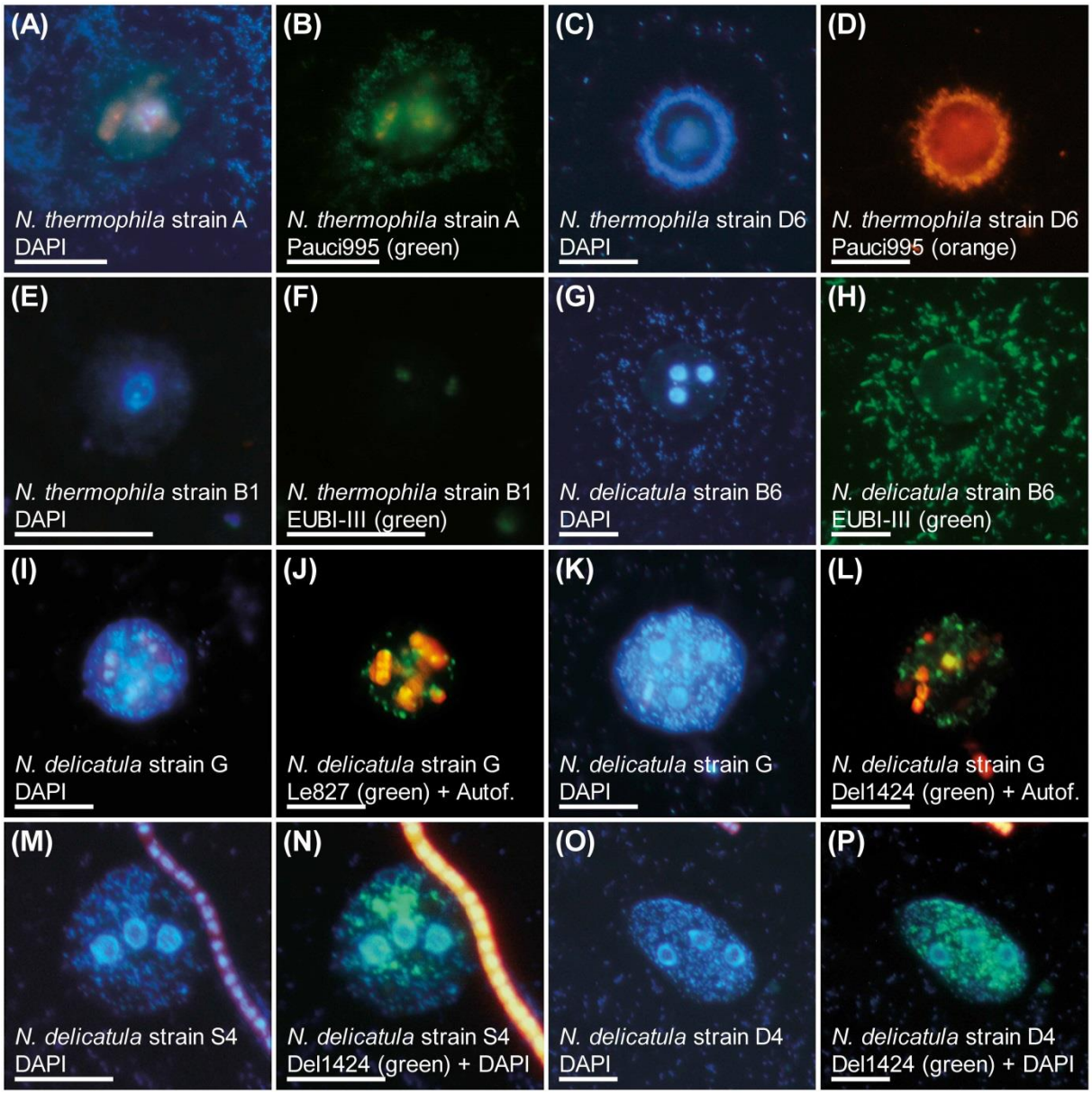

Figure 3 (Dirren & Posch)

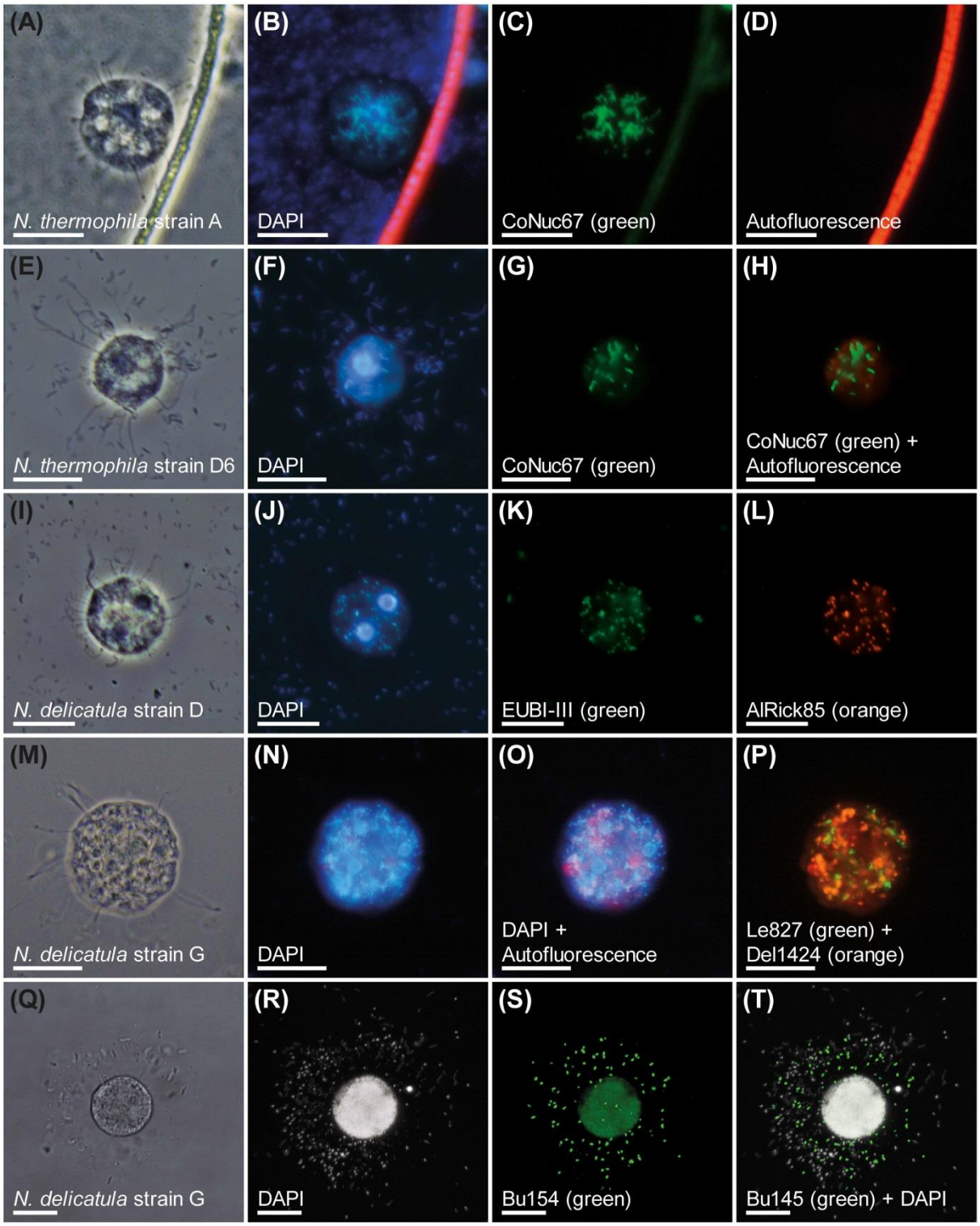

Figure 4 (Dirren & Posch)

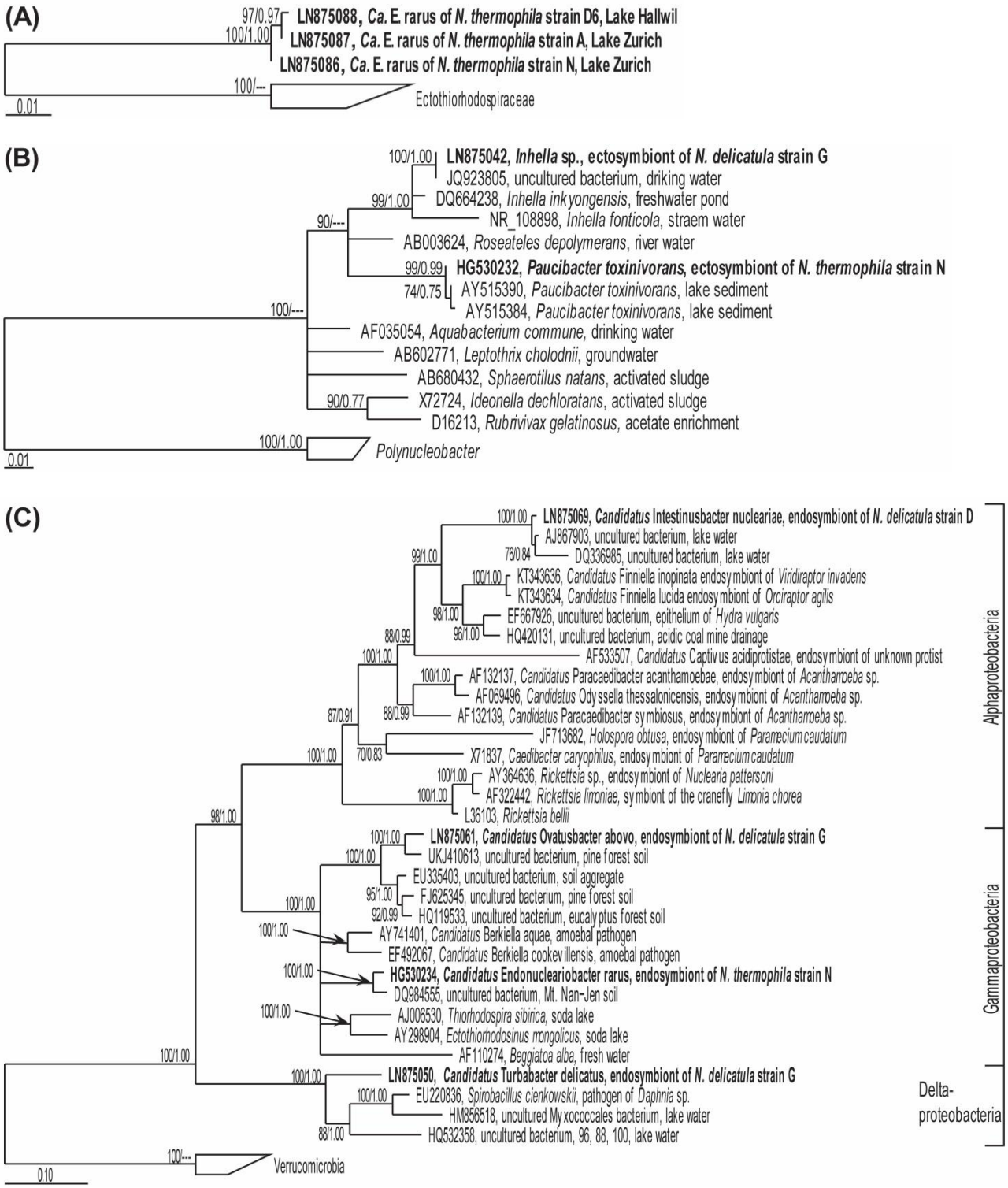

Figure 5 (Dirren & Posch)

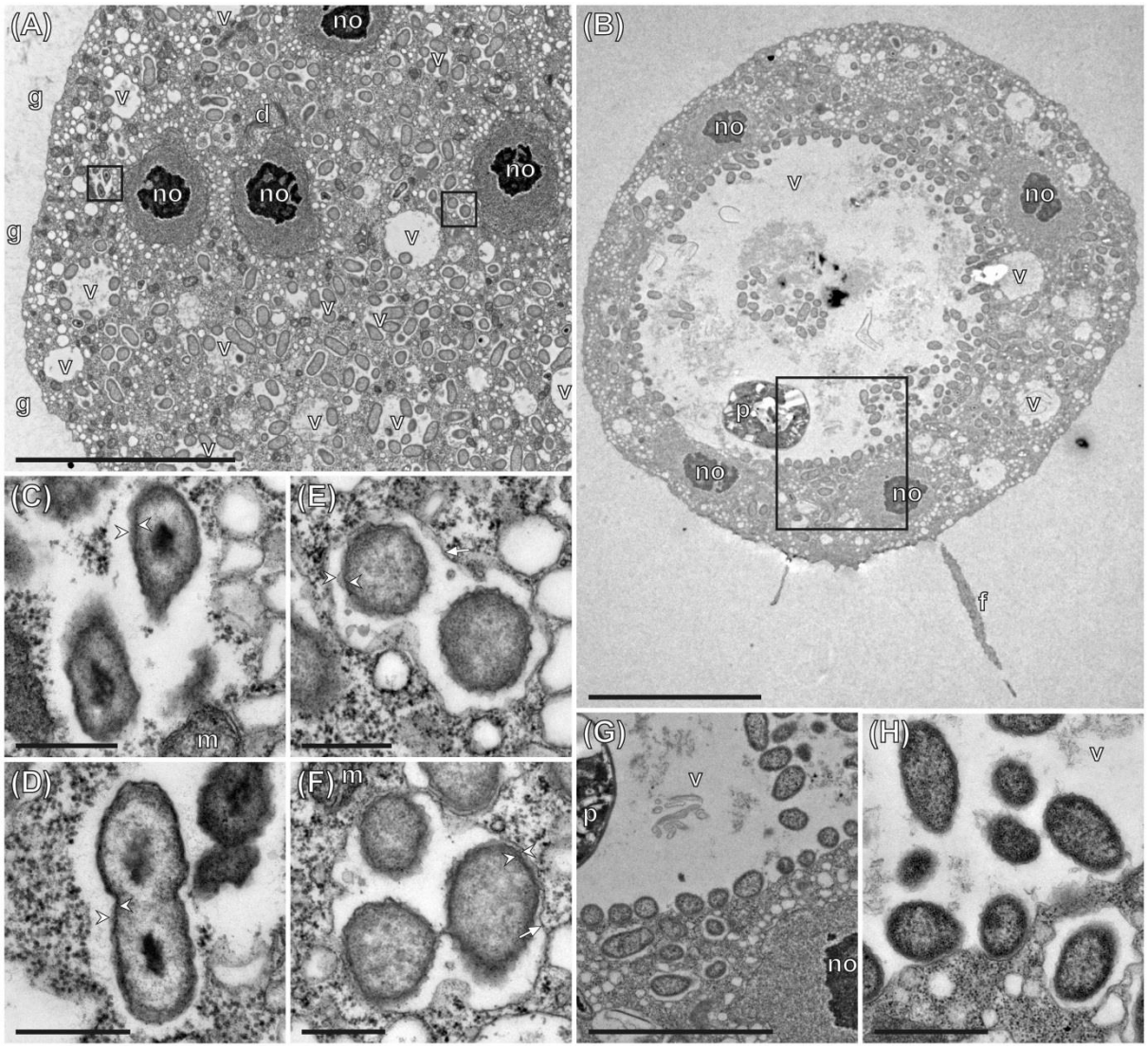

Figure 6 (Dirren & Posch)

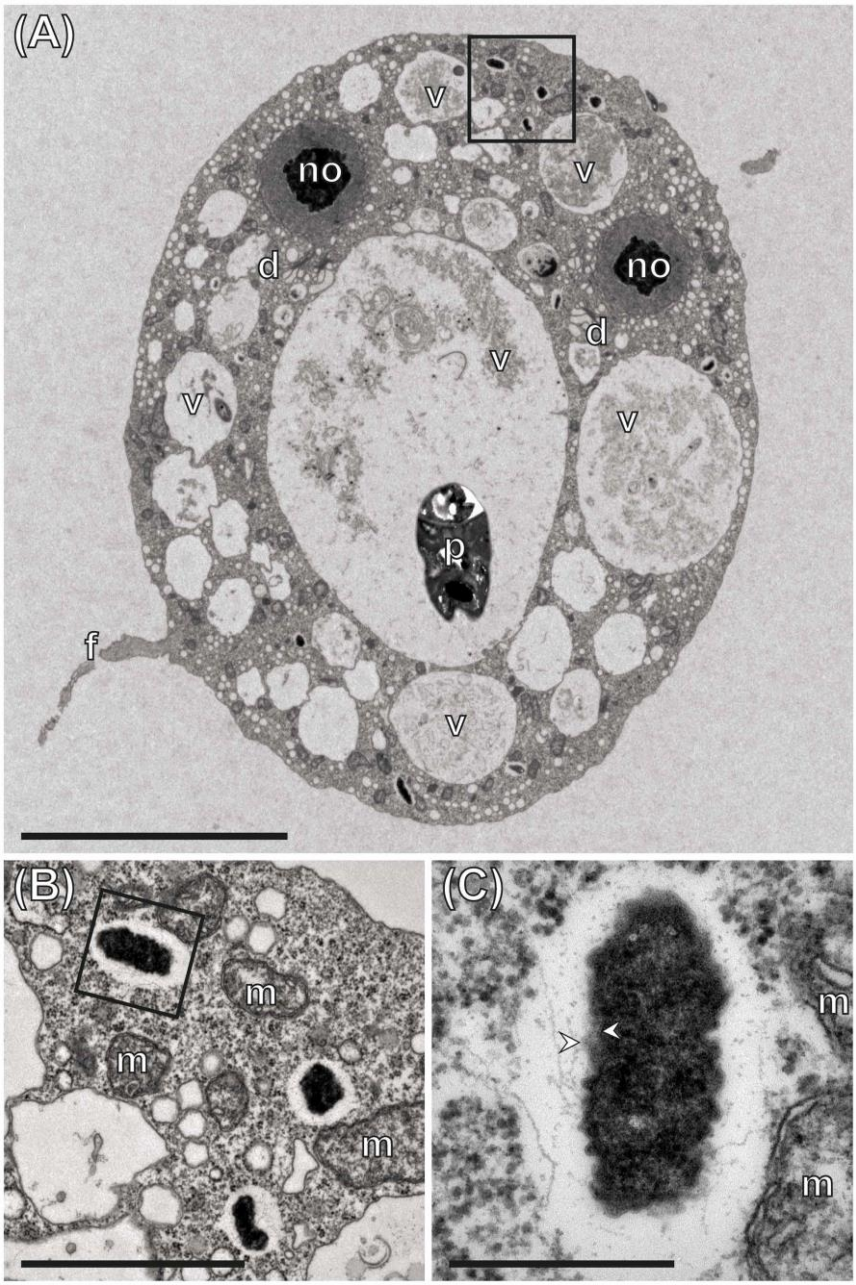

Figure 7 (Dirren & Posch)

Supplementary Figures S1-S3 to:

Promiscuous and specific bacterial symbiont acquisition in the amoeboid genus *Nuclearia* (Opisthokonta)

Sebastian Dirren and Thomas Posch[1]

Limnological Station, Department of Plant and Microbial Biology, University of Zurich,

Seestrasse 187, CH-8802 Kilchberg, Switzerland

[1]Corresponding author:

PD Dr. Thomas Posch

Limnological Station, Department of Plant and Microbial Biology, University of Zurich

Seestrasse 187, CH-8802 Kilchberg, Switzerland

Phone: 0041 44 634 9224

Fax: 0041 44 634 9225

e-mail: posch@limnol.uzh.ch

Supplementary Figure S1

Light microscopical pictures of 16 *Nuclearia* spp. isolates. (A) A syncytium originating from the fusion of cells contains multiple nuclei. (B) Eight cysts next to a *Planktothrix rubescens* (cyanobacteria) filament. (C) Elongated cell with an ingested *P. rubescens* filament. (D) Cyst having a 'perfect' spherical shape and a central nucleus. (E) Completely engulfed *P. rubescens* filament by a nucleariid cell. The organism formed two cell bodies which might lead to cell division. (F) Multinucleate cells sometimes show cell divisions which look like budding. Only a small part of the cell splits off. (G) Spherical individual with four visible nucleoli and radiating filopodia. Inside the cell an intact *P. rubescens* filament and remnants of already digested cyanobacteria can be seen. Ectosymbiotic bacteria are nicely arranged around the cell. (H) Club-shaped nucleariid cell with two ingested *P. rubescens* filaments (or possibly one filament which was bended). (I) Amoeboid cell with multiple nuclei. (J) Nucleariid cell which adapted an amoeboid form. The prominent nucleolus and multiple filopodia are visible. (K) Spherical cell with a large food-vacuole. Bacteria thriving in the cultivation medium are attached to the surface of the glycocalyx. (L) Syncytium with four nuclei and radiating filopodia. Spirochaete bacteria seem to be attracted by the amoeba but do not enter the glycocalyx. (M) Cyst with a thick cell wall. (N) Amoeboid organism with concentrated filopodia indicating the direction of locomotion. (O) Cyst with hardly visible nuclei and a thick cell wall. (P) Spherical cell (not a 'perfect' sphere) floating in the water column. (Q) A spherical shaped individual with radiating filopodia. (R) Amoeboid cell attached to the surface. A prominent nucleolus and thick, sometimes branched, filopodia can be seen. (S) Spherical individual with a hardly visible nucleolus. (T) Cell which adapted an amoeboid form. A completely ingested *P. rubescens* filament and the nucleolus can be detected. All pictures were taken with Differential Interference Contrast (DIC), except pictures (J) and (L), where phase contrast was applied. Scale bars indicate 20 µm.

Supplementary Figure S1

Supplementary Figure S2

Comparison of the nucleariid 18S rRNA genes. (A) Box plot of the pairwise distances (in %) of sequences from six 18S rRNA gene clone libraries (of six different isolates). Boxes: 25th to 75th percentiles; whiskers: 10th to 90th; crosses: 5th and 95th percentiles. (B) ML tree with posterior probabilities from BI; ML Bootstrap value / BI probability.All *N. delicatula* sequences from five different clone libraries, the sequence of *N. delicatula* (AF349563) and *N. simplex* (AF349566) / *N. moebiusi* (AF349565) as outgroup were used for phylogenetic reconstruction.

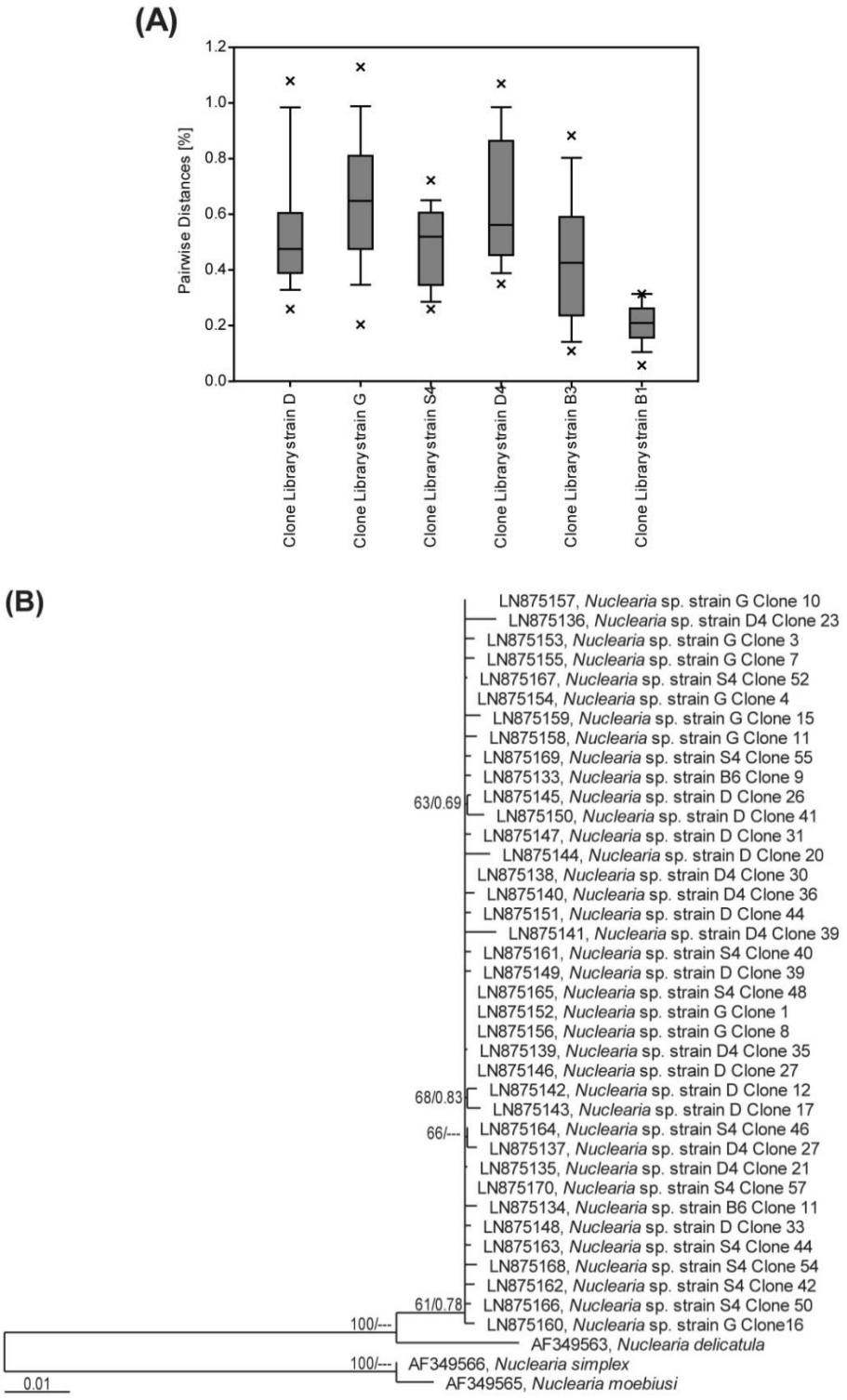

Supplementary Figure S2

Supplementary Figure S3

Phylogenetic analyses of two 16S rRNA clone libraries. ML trees with posterior probabilities from BI; ML Bootstrap value / BI probability. Branches with bootstrap values ≤ 50 were collapsed. Numbers in brackets represent the total number of partial sequences clustering with the respective group. Curly brackets represent the coverage of specific probes. Affiliations to higher taxonomic groups are indicated on the right side. Scale bar: number of nucleotide substitutions per site. (A) Phylogenetic tree of sequences from the clone library of the *N. delicatula* strain G culture and (B) of the *N. delicatula* strain D culture.

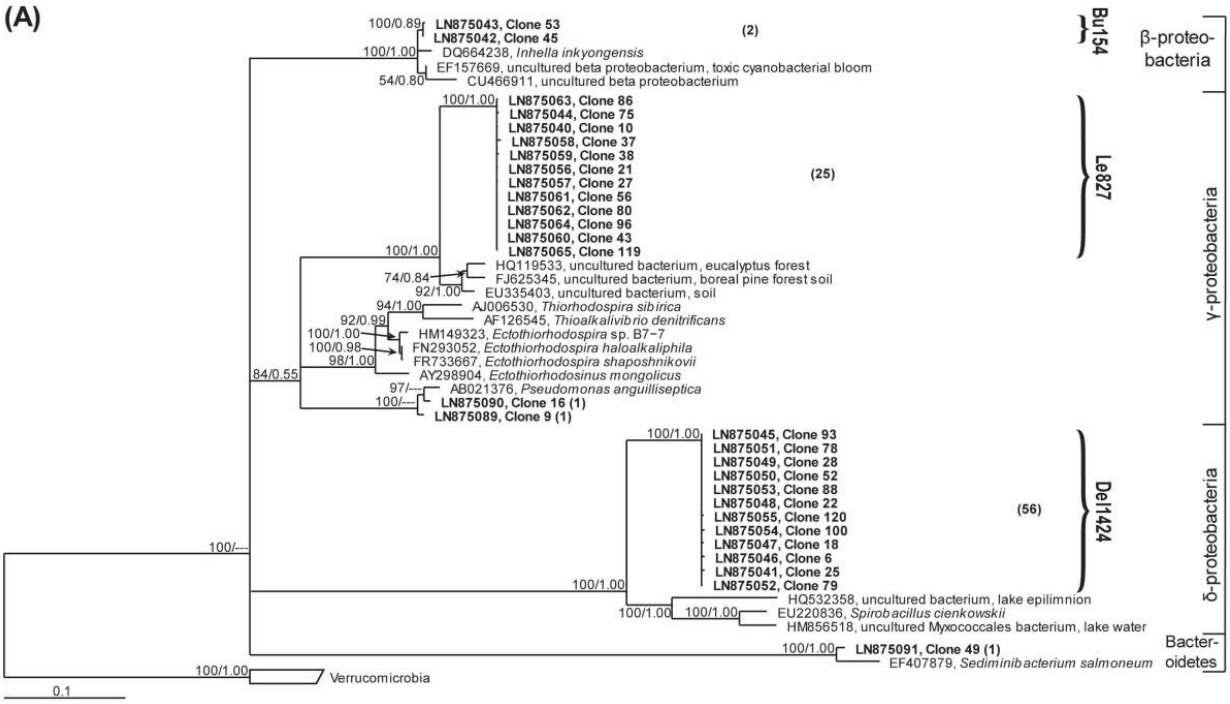

Supplementary Figure S3A

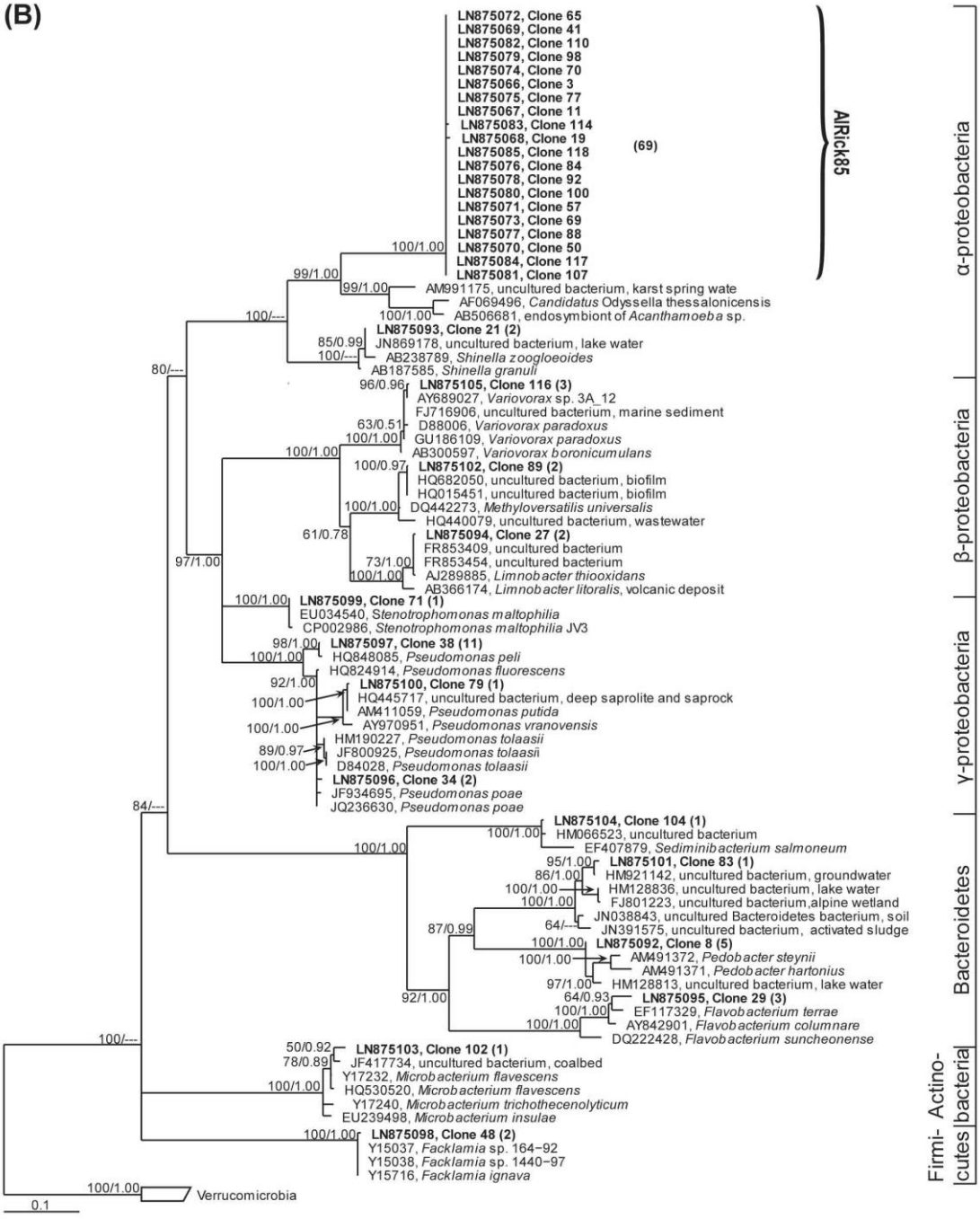

Supplementary Figure S3B